# Source-Adaptive Encoding Options for HDTV and NTSC

**By Kenneth A. Parulski, C. Bradley Hunt, and LeRoy E. DeMarsh**

*Television images originate from many sources, including video cameras, motion-picture film, and digital still graphics. This article describes how future all-digital high-definition television (HDTV) transmission systems and NTSC receivers can be designed to adapt to the frame rate, aspect ratio, color mode, and resolution of the signal source in a simple and cost-effective manner. This can provide improved picture quality or reduced transmission bandwidth requirements for image segments from certain sources. In HDTV transmission systems, the transmission coder operates at the source frame rate, for example, 24 frames/sec for film sources. The receiver frame store performs frame-rate conversion for the display. In high-end receivers, this processing can reuse the motion vectors transmitted by the HDTV coder. In NTSC receivers incorporating field stores and progressive scan displays, source-adaptive processing allows perfect interlace to progressive scan conversion and luminance/chrominance decoding for still images, and improved decoding of images from motion-picture film. To make these methods more efficient, "origination-source ID" data is incorporated into the video signal during post-production.*

Television uses images from many sources, some of which are listed in Fig. 1. Many TV programs originate from NTSC video cameras, of course, but for sports or news from Europe, standards-converted PAL or SECAM signals are used. Computer graphic stills are used for short segments, such as weather maps, and for much longer segments on some cable promotional and home shopping channels. Because they include graphics and text, these can be some of the most demanding images. Finally, both classic movies and most prime-time entertainment programs originate on motion-picture film.

Future HDTV systems will certainly use all of these sources, as well as HDTV cameras based on one or more of the proposed HDTV production standards. This article describes how TV systems can adapt to the source to provide better pictures or even allow multiple programs in one channel. By sending a few bits of data describing the source, the TV channel can be used more efficiently. Many of the basic ideas described in this article were developed by the Advanced Television Research Program at MIT.[1,2]

## NTSC Scanning Standard

The NTSC color television standard was developed almost 50 years ago.[3] Because inexpensive memory did not exist, the scanning beams in all home receivers had to be synchronized to the camera in the studio. All of the cameras and receivers had to operate at the same line and field frequencies, and scan the same spot at the same instant, in order to display properly synchronized images. To minimize display flicker while conserving transmission bandwidth, interlaced scanning was employed. Interlace scanning means that only half of the lines in the image are transmitted during each video field period.

Figure 2 is a simplified diagram of today's NTSC television system. In the television studio or post-production house, images from 24 frame/sec film and 50 field/sec European programs are all converted to the 525-line, 59.94 field/sec, 2:1 interlaced NTSC format, before transmission. The conversion is done using a digital frame-rate converter in the telecine, or a digital standards converter. Conventional receivers display the decoded NTSC signal using the same scanning standard. However, a small but growing number of receivers use different display standards.

Certain receivers, sometimes identified as improved-definition television (IDTV) receivers, use digital fieldstores to convert the interlaced NTSC transmission signal to a progressive scan signal.[4] IDTV receivers use line-doubling techniques in order

| Video cameras | Stills & graphics | Motion picture film |
|---|---|---|
| ■ NTSC | ■ CGs | ■ Monochrome |
| ■ PAL | ■ Still stores | ■ Color |
| ■ SECAM | ■ Slide scanners | ■ 35mm |
| | | ■ 16mm |

*Figure 1. Television image sources.*

Presented at the 133rd SMPTE Technical Conference (paper no. 133-33) in Los Angeles on October 27, 1991. Kenneth A. Parulski (who read the paper) and C. Bradley Hunt are with Eastman Kodak Co., Rochester, NY 14650. LeRoy E. DeMarsh is retired from Eastman Kodak Co. Copyright © 1992 by the Society of Motion Picture and Television Engineers, Inc.

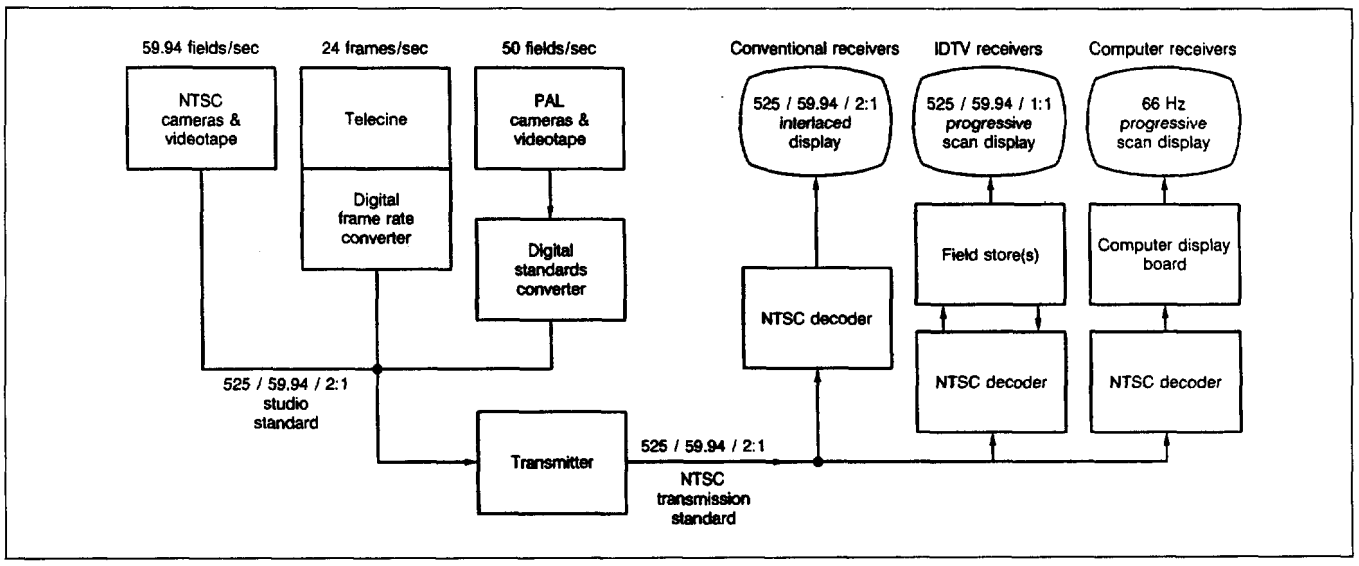


*Figure 2. Current NTSC television system.*

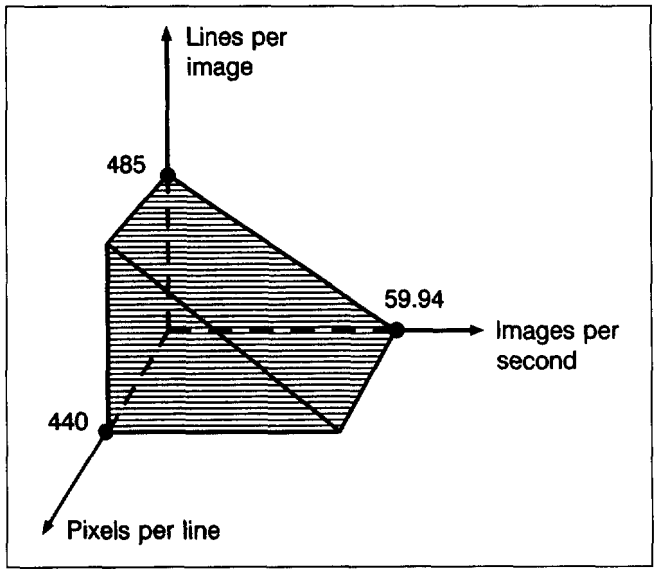


*Figure 3. NTSC origination and NTSC transmission.*

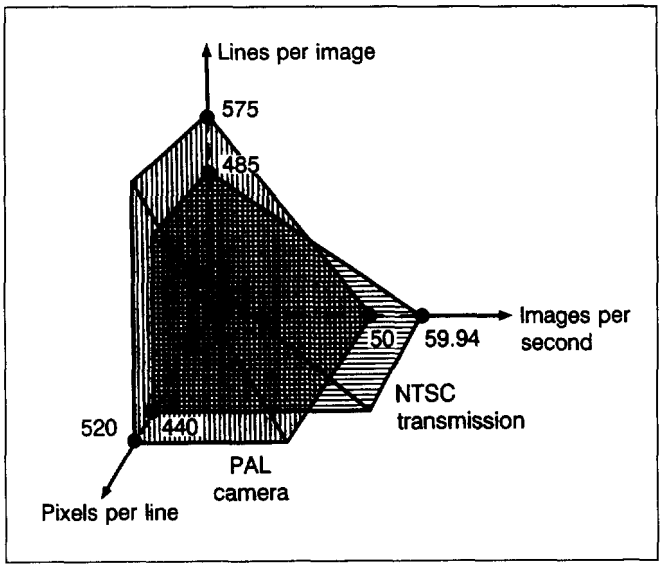


*Figure 4. PAL origination and NTSC transmission.*

to display all of the video lines at a 59.94-Hz frame rate. Some plug-in boards for desktop computers include TV tuners and NTSC decoders. These boards convert from the NTSC scanning standard to the computer's display rate, for example, 66 Hz. Thus, in today's NTSC world, even though the 59.94 field/sec interlaced scanning format is always used for transmission, other frame rates and scanning formats are often used for origination and display.

## Transmission Efficiency for Different Image Sources

All six of the advanced television (ATV) systems scheduled for testing by the Advanced Television Test Center (ATTC) in Washington, D.C., use one or more frame stores in both the transmitter and receiver. This allows the characteristics of the source, channel, and display to be decoupled. Different transmission frame rates can be used for images with different origination frame rates. This can significantly improve the transmission efficiency. A simple way of considering the transmission efficiency is to use three-dimensional plots. The vertical dimension of the plot gives the number of lines per image, the horizontal spatial dimension of the plot gives the number of pixels per line, and the temporal dimension of the plot gives the number of images per second.

Figure 3 shows an alias-free spatiotemporal volume for an NTSC luminance signal.[5] There are approximately 485 active lines/frame. The 4.2-MHz bandwidth corresponds to about 440 pixels/line, disregarding the Kell effect.[6] The field rate is about 60 Hz. The triangularly shaped volume shown in Fig. 3 is one of several possible alias-free volumes for interlaced signals.[7] The size of the enclosed volume is directly related to the transmission bandwidth.

The output of an NTSC video camera matches the NTSC transmission bandwidth. However, the standards-converted output of a PAL camera does not match the NTSC transmission bandwidth, shown in Fig. 4. Only the cross-shaded areas common to both volumes make it to the receiver. NTSC transmission limits the vertical and horizontal resolution of the PAL image, shown in the vertically shaded regions. It also provides additional temporal resolution, shown in the horizontally shaded regions, which is not used. This means that

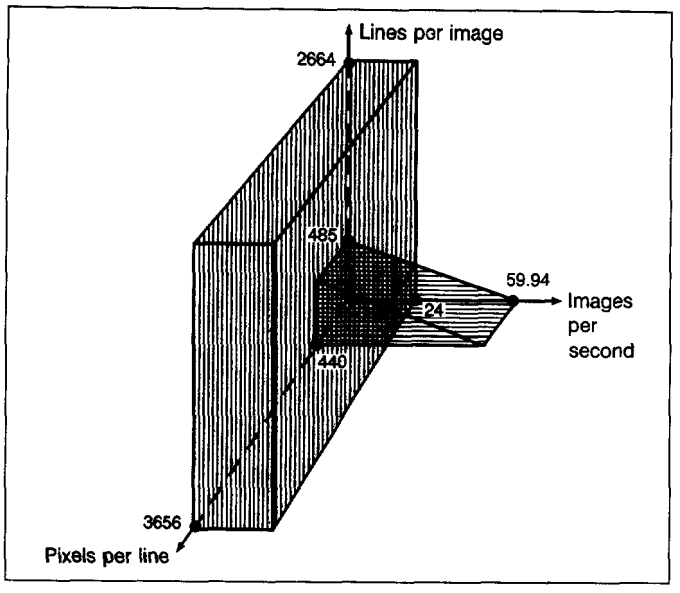


*Figure 5. Motion-picture origination and NTSC transmission.*

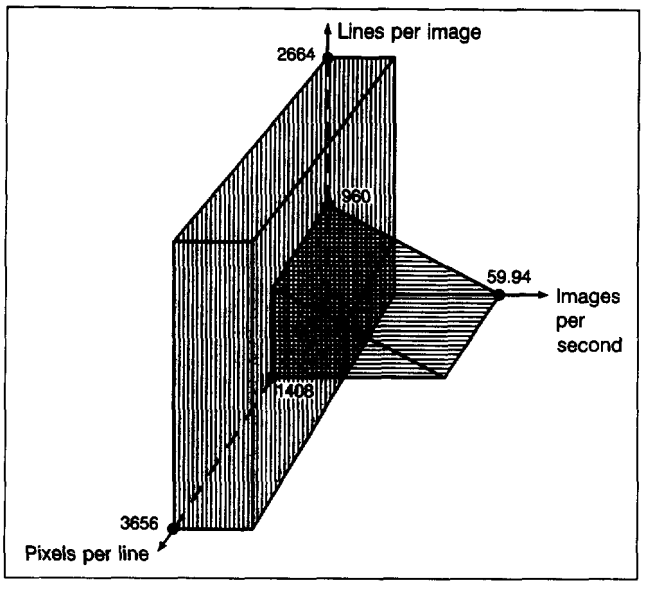


*Figure 6. Motion-picture origination and HDTV transmission.*

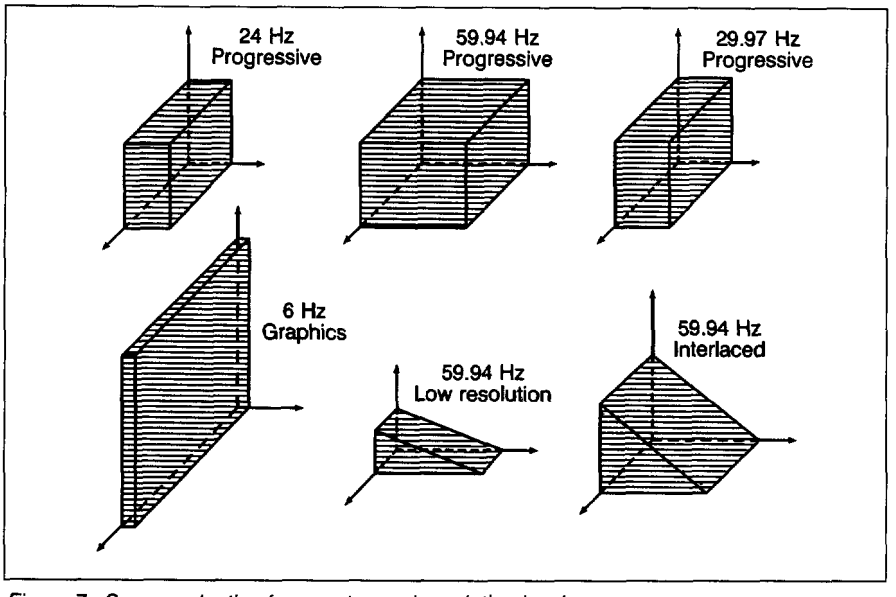


*Figure 7. Source-adaptive frame rates and resolution levels.*

part of the valuable transmission bandwidth is wasted.

Figure 5 shows roughly the volumes for motion-picture film origination and NTSC transmission. Film does not have lines or pixels, of course. For illustration purposes, Fig. 5 uses the 35mm Academy aperture scanning parameters from a high-resolution electronic intermediate system for motion-picture film.[8] The NTSC channel severely restricts the vertical and horizontal limiting resolution that can be transmitted from film-originated images. NTSC also provides unused temporal resolution, which is wasted when transmitting 24 frame/sec film.

Note that the limiting spatial resolution of typical images scanned from 35mm motion-picture film is not necessarily equal to the film spatial scanning parameters (Fig. 5). Rather, the scanning parameters set an upper bound on the limiting resolution. This is also true of the scanning parameters for a video camera. The limiting spatial resolution of any image-capture system is affected by many factors, including the modulation transfer functions of the camera lens and the film or image sensor.[9,10]

## Source-Adaptive Encoding Parameters

The design of a digital HDTV system presents many alternatives. The conventional approach is to make the transmission system support only a single, fixed format with a set frame rate and a set number of lines per frame. All sources are then translated to this format before transmission. Figure 6 shows the volumes for film origination and a 1050-line, 59.94 field/sec, 2:1 interlaced HDTV transmission format. Compared to NTSC, an HDTV system can send a much higher-resolution film image in the same 6-MHz channel, because of compression. However, motion-picture film still has greater spatial resolution and lower temporal resolution than the HDTV standard, so a significant part of the transmission bandwidth is used inefficiently.

Moving to an all-digital HDTV transmission standard provides an opportunity to reexamine key system attributes. The flexibility inherent in digital systems makes it easy to adapt the transmission format to the image source. This is critically important, because it allows the transmission bandwidth to be used as efficiently as possible for all sources. It also allows the system to be compatible with future origination sources, such as 1050-line progressive scan video cameras. Such high-line-rate, progressive scan cameras are not technically feasible at the present time,[11] but may be available by the time HDTV receivers achieve significant penetration in the consumer market.

Using source-adaptive encoding, an HDTV system can be designed to support a small number of different source frame rates and sampling structures. Some options, shown in Fig. 7, include progressive scanning modes at 24 frames/sec, as well as

higher frame rates such as 29.97 Hz and 59.94 Hz. Other possibilities include a 2000-line low frame rate graphics mode, and an "NTSC resolution" interlaced scanning mode. For modes with small volumes, such as the 24-Hz film mode and the NTSC resolution mode, multiple programs might be accommodated in a single 6-MHz TV channel. The mode is indicated by a source ID code transmitted once per frame.

The Kodak Photo CD System[12] provides a useful model of how source-adaptive HDTV might accommodate multiple resolution levels in a hierarchical format. In the Photo CD system, still-format film images are scanned using 2048 lines/picture height (ph) and stored on a compact disc. The format includes many resolution levels, shown in Fig. 8, to allow rapid access for various applications. For HDTV, a three-level approach, including a BASE level providing NTSC resolution, a 4-BASE level providing HDTV resolution, and a 16-BASE level for super-high-resolution stills and graphics may be appropriate. For compatibility with NTSC, the BASE level could use 485 lines/ph.

The picture aspect ratio is a key source parameter. NTSC has a fixed aspect ratio of 4 units wide by 3 units high. When a widescreen movie is shown in its original aspect ratio, a black letterbox is added to the top and bottom of the picture. Transmitting these black bars obviously wastes bandwidth. In conventional HDTV, the transmission format also has a fixed aspect ratio, which is 16:9. When 4:3 images, from upconverted NTSC or classic movies, are transmitted in their original aspect ratio, black sidebars must now be added. This again wastes substantial bandwidth. Using source-adaptive encoding, only the actual image information needs to be transmitted. The source ID indicates which aspect ratio is being used, and the black bars are added by the receiver.

Another important source parameter is the color mode. Many classic movies and early TV shows were produced in black and white. Without source-adaptive encoding, an HDTV system wastes bandwidth by sending zero-level color-difference signals for these programs. With source- adaptive encoding, a single bit is transmitted to

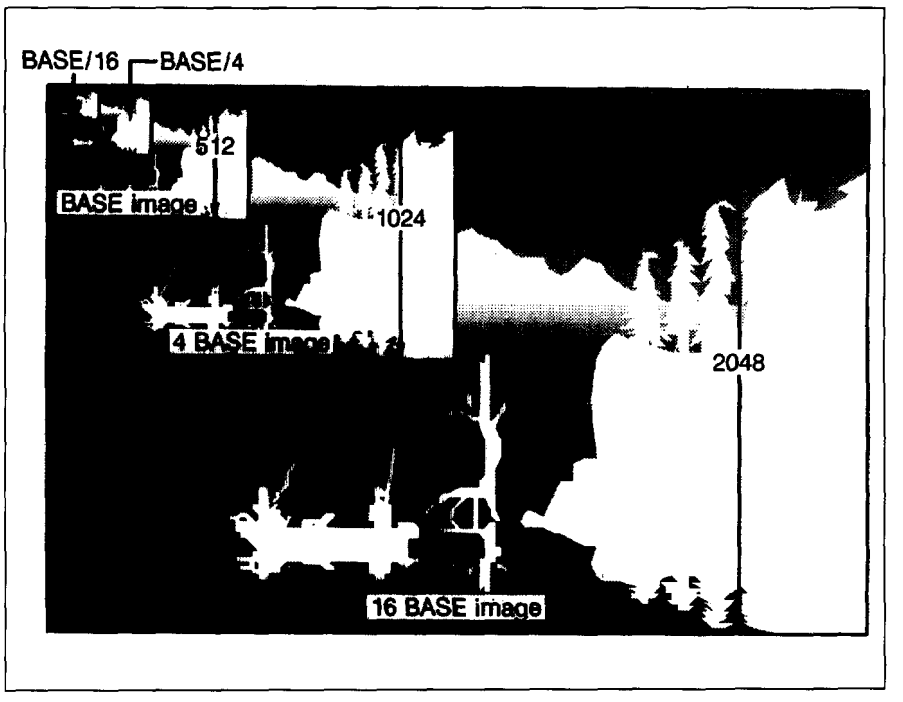


*Figure 8. Kodak Photo CD System resolution hierarchy.*

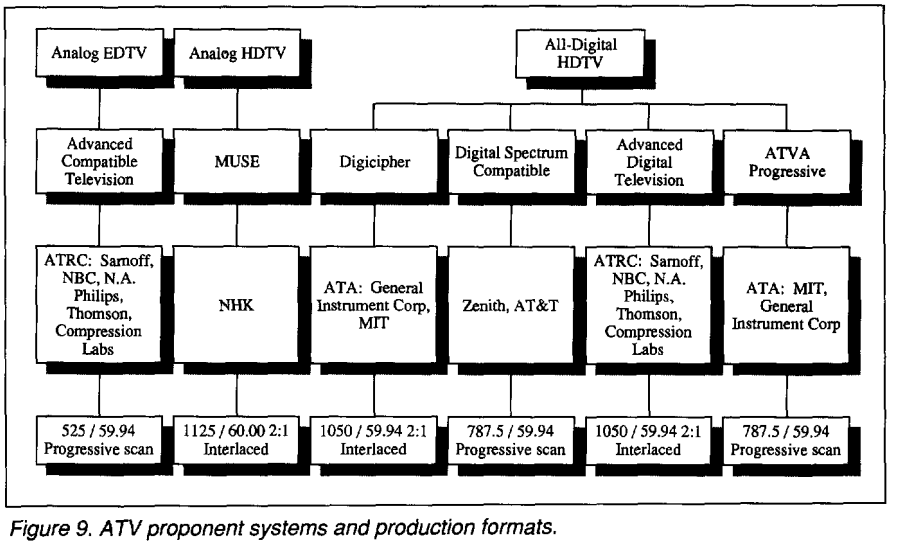


*Figure 9. ATV proponent systems and production formats.*

*Figure 10. Original frame of simulated motion sequence.*

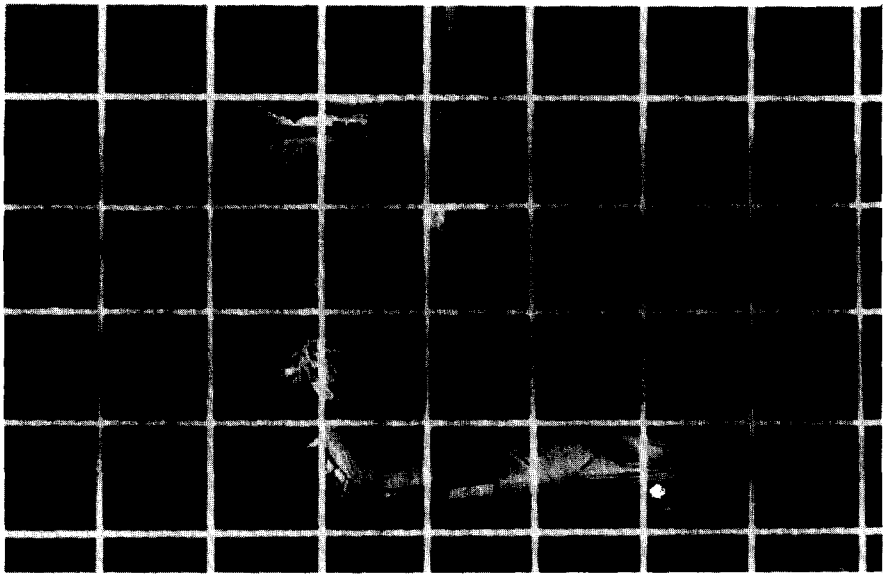

*Figure 11. Blocks of original frame of sequence.*

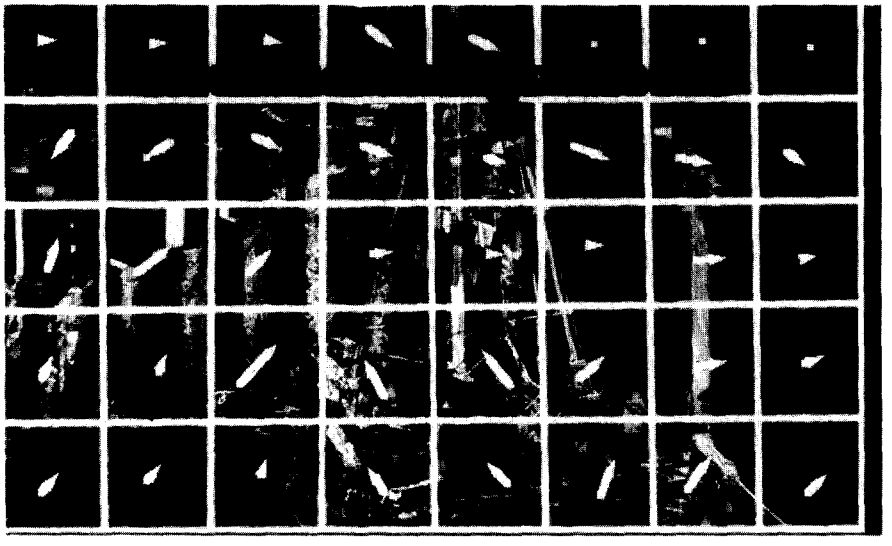

*Figure 12. Motion vectors and residual image blocks.*

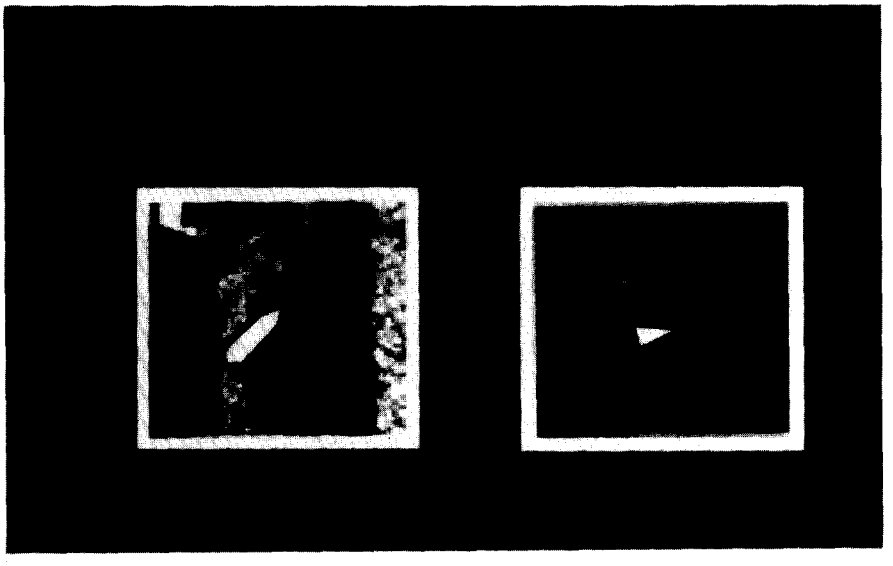

*Figure 13. Enlarged view of residual image blocks: (a) significant change; (b) little change.*

indicate that the image is black and white. It is not necessary to transmit the color-difference signals, and the additional bandwidth can be used to improve the quality of the program by reducing coding artifacts.

## All-Digital HDTV Transmission Systems

Of the six proposed ATV systems shown in Fig. 9, four use all-digital transmission.[13-16] These four systems use very similar image-compression techniques, which can be more easily understood using simple photographic illustrations. Figure 10 shows a cropped section from one frame of a simulated motion sequence, where the camera is zooming in while panning to the right. The four compression systems compute the differences between blocks of the current frame, shown inside the white grid overlay in Fig. 11, and spatially shifted blocks from the previous frame.

The shift directions and magnitudes of each block, known as motion vectors, are shown as arrows in Fig 12. The motion vectors describe the average motion that occurred within each block of the image during the time between the current frame and the previous frame. The strange-looking image within the white grid in Fig. 12 shows the difference between the blocks of the current image frame and the shifted blocks of the previous (delayed) frame. This difference image is called the "residual." The residual is compressed, using the discrete cosine transform (DCT) or multiscale subband filters, and transmitted to the receiver along with the motion vectors.

Figure 13 shows the residuals from two different blocks. In Fig. 13a the motion vector and residual is large, because there was a significant change in this part of the image from one frame to the next. The block in Fig. 13b shows that when there is little change, the residual is small. More bits of data are needed to code the larger residuals, of course. Since the data rate of the TV channel is limited, images with many large residuals must be coarsely quantized. This causes artifacts in the decoded image.

## HDTV Systems Using Source-Adaptive Encoding

Figures 14 and 15 compare a digital HDTV transmission system, both

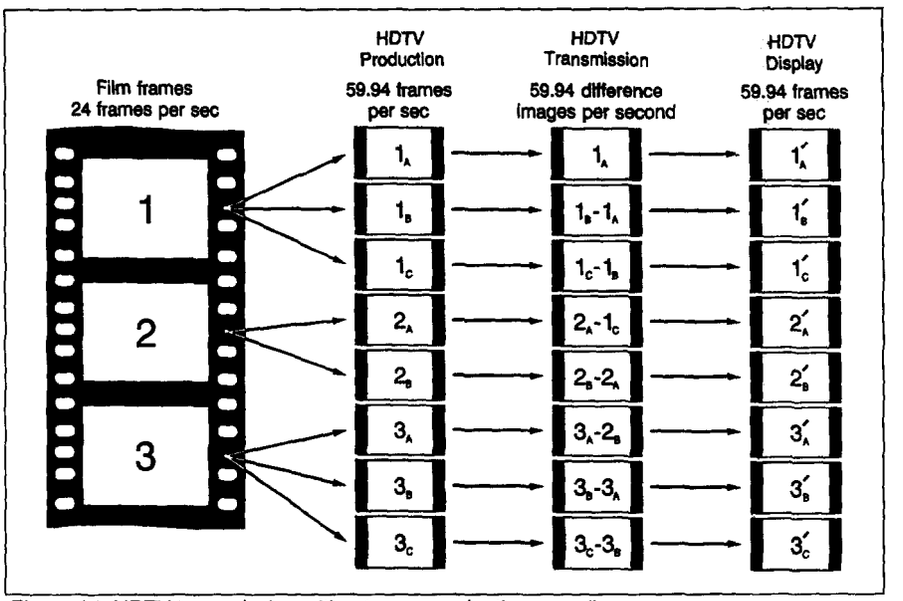


*Figure 14. HDTV transmission without source-adaptive encoding.*

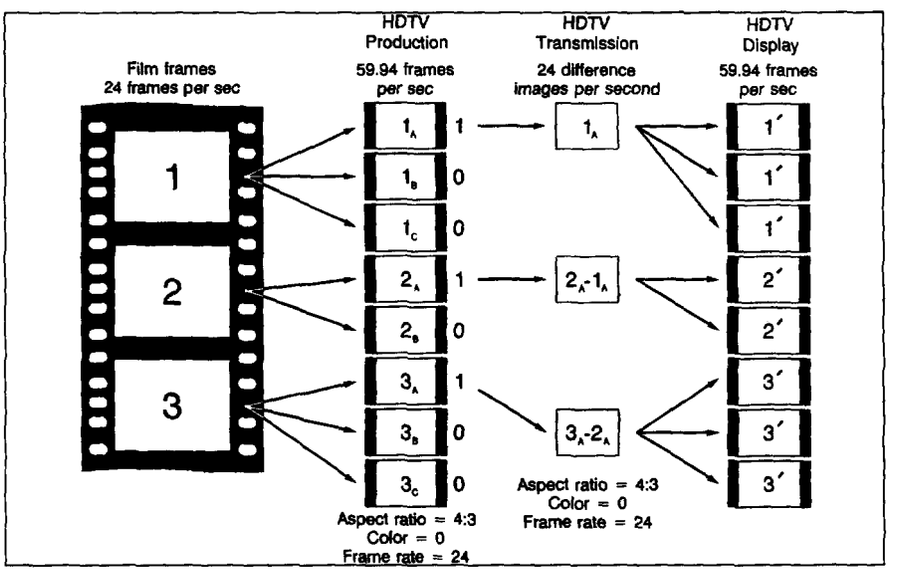


*Figure 15. HDTV transmission using source-adaptive encoding.*

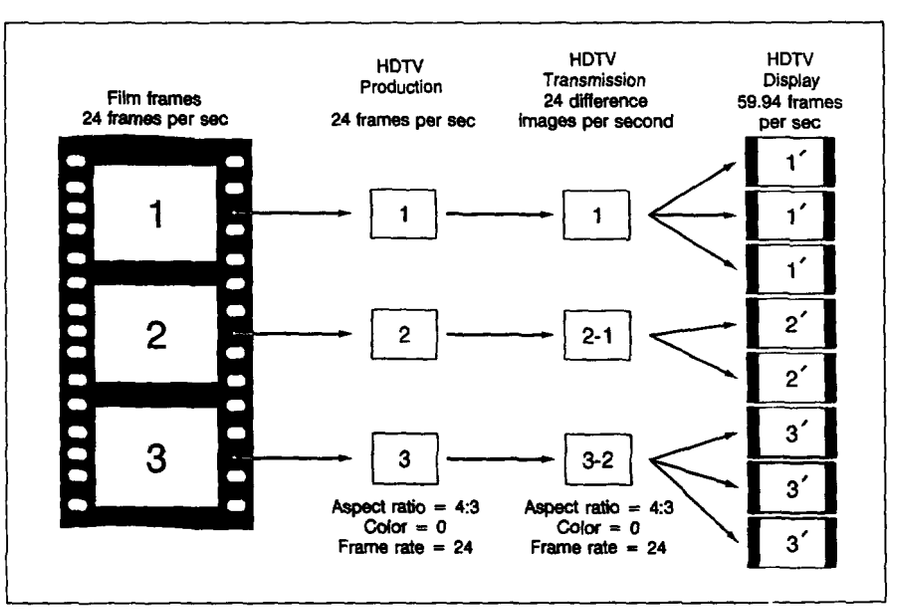


*Figure 16. HDTV production and transmission using source-adaptive encoding.*

with and without source-adaptive encoding, from origination through display. For source material, consider the black-and-white movie, *Casablanca,* which was shot in a 4:3 aspect ratio, at 24 frames/sec. First consider Fig. 14, which does not use source-adaptive encoding. The film is transferred on a telecine, which converts it to a 59.94 frame/sec rate using 3:2 pulldown, so that the odd film frames are repeated three times and the even film frames are repeated twice.

At the transmitter, the film images are coded no differently than if they came from a video camera. This means that three difference images are used to code a single even film frame, and two difference images are used for each odd film frame. When multiple residual frames are used to code the same film frame, a significant fraction of the transmitted bits are wasted. The first residual, from the new real film frame, contains most of the energy and therefore possible artifacts. The image improves over the next one or two residual frames. However, there is much redundancy in using multiple motion vectors and multiple coded residuals for each film frame. Because the system assumes a 16:9 aspect ratio color image, additional bits are wasted sending black sidebars and color-difference signals, which contain no meaningful information. These are small but not necessarily zero-level signals, since they may include analog noise from the post-production process.

Figure 15 shows a digital HDTV system with source-adaptive encoding. The 24 frame/sec film is again transferred on a telecine using 3:2 pulldown, to provide a 59.94-Hz frame rate. In addition, origination-source ID data bits, provided in a manner similar to SMPTE time code data, indicate real film frames, the 4:3 aspect ratio, and black and white. At the transmitter, only the differences between the real film frames, identified by the origination source ID, are computed. Now, 2.5 times as many bits are available for coding each residual frame. This allows the image to be transmitted with fewer artifacts. On the other hand, the extra bits could instead be used to transmit a higher-resolution image, expand the coverage area, or perhaps transmit multiple

*Figure 17. Brief 24 frame/sec motion film sequence: (a) first original frame; (b) last original frame.*

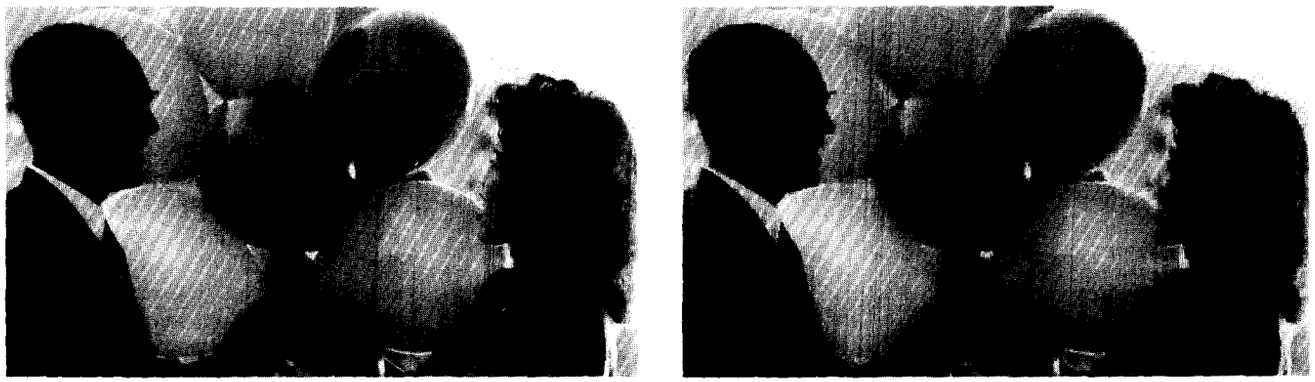

*Figure 18. First frame of sequence: (a) first compressed frame using source-adaptive encoding; (b) first compressed frame without source-adaptive encoding.*

programs in one 6-MHz channel. Since the origination-source ID also indicates the aspect ratio and color mode, the sidebars and color-difference signals are not transmitted. In the receiver, each film frame is displayed multiple times, to prevent flicker. This requires a digital frame memory in the receiver. Since the four systems all use receivers with at least one full frame memory, performing the 3:2 pulldown in the receiver adds essentially no cost.

The main differences between the four all-digital HDTV transmission systems are the choice of studio standards and the details of the algorithms used to calculate the motion vectors, code the residuals, and transmit the digital data. These systems can easily and inexpensively incorporate the source-adaptive processing described. In fact, source-adaptive frame-rate features are included in the Digicipher system[13] and the ATVA Progressive system.[14] The Digital Spectrum Compatible Systems[15] includes a special film mode used for 24 and 30 frame/sec source material, while maintaining a 60 frame/sec transmission frame rate. A modified buffer control algorithm is used to allocate more data bits to the quantizers used to code the residuals corresponding to real film frames and fewer data bits to the repeated frames.

Source-adaptive encoding can be used in HDTV production as well as transmission, as shown in Fig. 16. Here, the film is transferred on a telecine and recorded using a 24-Hz frame rate. This obviously reduces the amount of videotape needed. The rest of the system is the same as described earlier in reference to Fig. 15.

## Source-Adaptive Encoding Simulation

Figures 17a and 17b show the first and last frames of a brief 24 frame/sec film sequence, with roughly 720 lines by 1280 pixels. This original sequence was processed by John Apostolopoulos at MIT to simulate the MIT ATVA Progressive system, both with and without source-adaptive encoding.

Figures 18a and 18b show the first frame of the sequence, after compression. Figure 18a uses source-adaptive encoding, while Fig. 18b does not. To demonstrate the quality differences clearly, compression to 0.16 bits/pixel was used. This bit rate allows two programs to fit into one 6-MHz TV channel. Notice the blocking artifacts in Fig. 18b. The artifacts are very pronounced, because this is the first frame following a scene change. Figures 19a and 19b show the last frame of the sequence, after compression. Figure 19a uses source-adaptive encoding and Fig. 19b does not. The differences here are much smaller, because the frame-to-frame differences in the sequence are relatively small.

## Receiver Implementation of Source-Adaptive HDTV Features

One key consideration in deciding which source-adaptive features to incorporate into an HDTV transmission standard is the cost of the additional receiver circuitry needed to implement the feature. Since even the lowest-cost HDTV receivers must be designed to obtain viewable images from all standardized source formats, the cost of the additional circuitry must be minimal. The cost of an HDTV receiver depends primarily on

*Figure 19. Last frame of sequence: (a) last compressed frame using source-adaptive encoding; (b) last compressed frame without source-adaptive encoding.*

the cost of the CRT display and the frame memory, and the cost differences between the four all-digital systems are relatively small.[17] Adding some source-adaptive features, such as the source-adaptive aspect ratio and source-adaptive color mode, require only minor changes in the receiver control circuitry in order to provide the proper black borders and the zero level color-difference signals. The source-adaptive frame rate conversion circuitry can utilize the same full frame memory included in the receivers of the four all-digital systems, although the memory control circuit may be slightly more complex, since the memory must now operate at various input frame rates. The number of allowable frame rates and aspect ratios has little impact on the receiver cost.

High-end source-adaptive HDTV receivers may include additional processing to provide improved picture quality. For example, the use of 3:2 pulldown to perform 24 Hz-to-60 Hz conversion in the telecine, as shown in Fig. 14, or in a source-adaptive receiver, as shown in Figs. 15 and 16, can cause motion judder. Motion-compensated frame-rate conversion can eliminate motion judder. Such processing is normally prohibitively expensive in a receiver because of the computations needed to calculate motion vectors. In the all-digital HDTV systems, the expensive transmitter has already calculated the motion vectors and sent them to the receiver.

In top-of-the-line receivers, these same vectors can be reused for frame-rate conversion. The simple algorithm shown in Fig. 20 performs 24 Hz-to-60 Hz motion-compensated frame-rate conversion. The receiver decodes and displays film frame 1, using the motion vectors sent with each residual block to perform the normal decoding process. But rather than discarding the motion vectors and repeating film frame 1 for the next two video frames, it displays slightly shifted versions of film frame 1. Each block within film frame 1 is shifted by an amount equal to the scaled motion vector for that block. The scale factors are multiples of 0.4, in order to provide the proper temporal alignment of the film frames, which have a frame rate equal to 40% of the video display rate. Instead of a 60-Hz display rate, some high-end sets could use a higher rate, such as 72 Hz, to more completely eliminate flicker.[18] In these receivers, the transmitted motion vectors would be used to upconvert video camera sources, as well as film sources.

The cost of the additional receiver circuitry needed to implement source-adaptive resolution depends on the number of resolution levels allowed, and on how the different resolution levels are mapped to the display screen. If the standard allows the transmitted image to use an arbitrary number of lines or pixels to represent a full screen image, the decimation/-interpolation circuitry required in the receiver will be quite complex.

The required processing can be greatly simplified by using a limited number of resolution levels that are binary multiples of the base resolution. The base resolution could equal the number of active scanning lines in the NTSC standard. The decimation or interpolation could then be accomplished by truncating or zero-padding the high-order DCT or subband coefficients that represent the residual image. This should require only minor modifications to the DCT or subband decoder in the receiver. Of

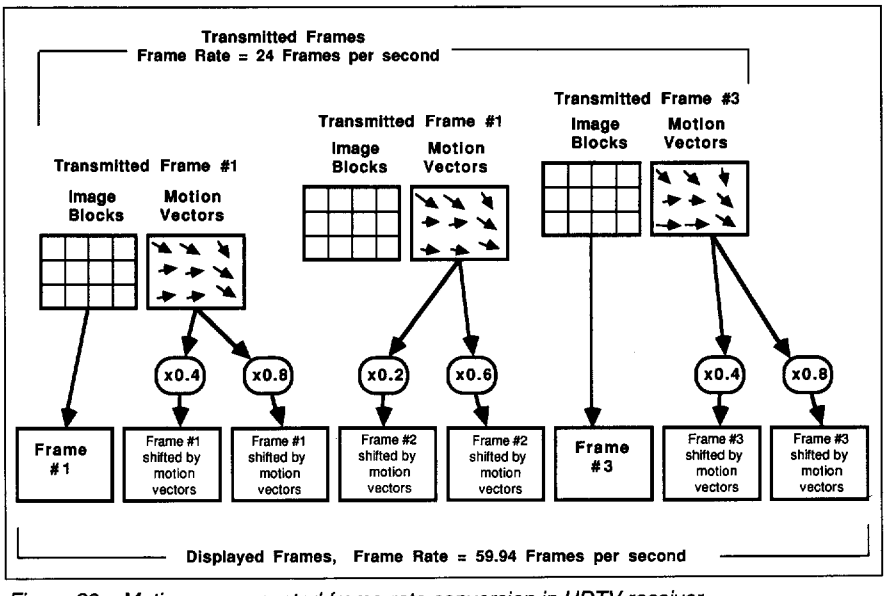


*Figure 20. Motion-compensated frame-rate conversion in HDTV receiver.*

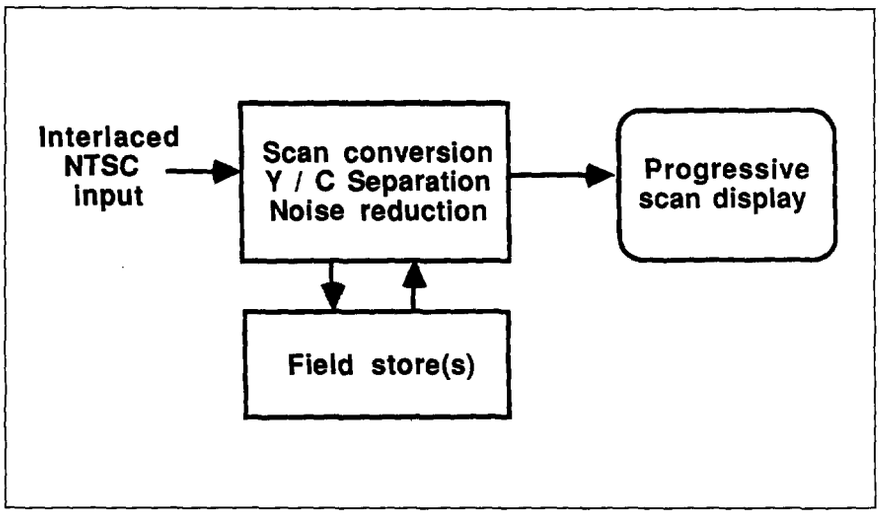


*Figure 21. Conventional IDTV receiver.*

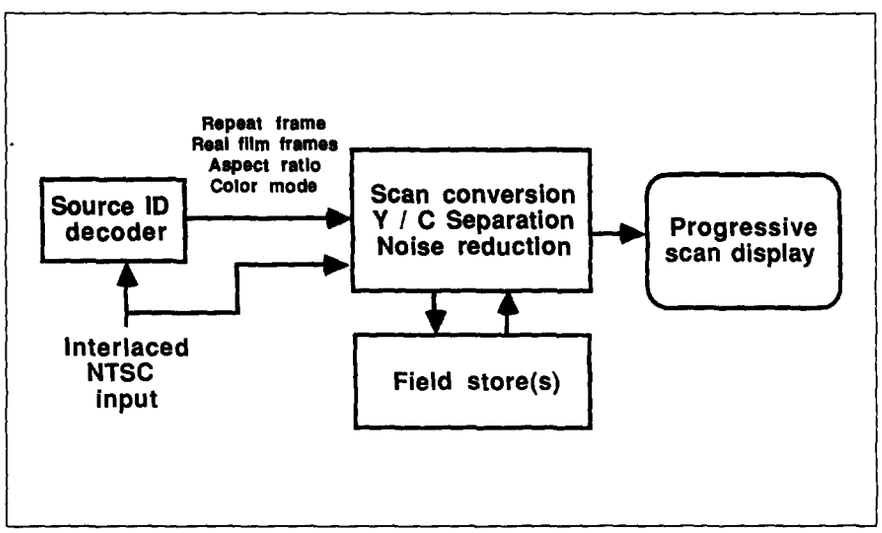


*Figure 22. Source-adaptive HDTV receiver.*

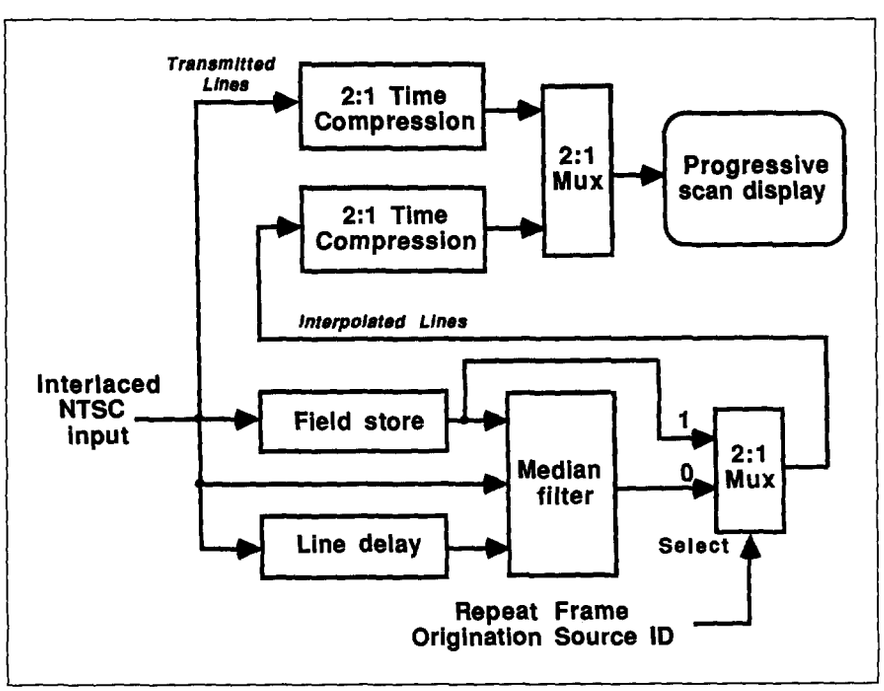


*Figure 23. Progressive scan conversion for repeat frames.*

course, high-end HDTV receivers could utilize more sophisticated interpolation techniques. If the resolution of the transmitted image, for example using the graphics mode, was greater than the addressable display resolution, the receiver would simply display the image at the lower-resolution level provided by the display. Thus all HDTV receivers could display an image transmitted in this mode, but only the top-of-the-line HDTV receivers would allow the full resolution of the graphics mode image to be displayed, or perhaps printed.

## Source-Adaptive Processing for NTSC

In another extension of this concept, source-adaptive processing can improve images from today's NTSC format. Current IDTV receivers use field stores for interlace to progressive scan conversion, luminance/-chrominance (Y/C) separation, and noise reduction (Fig. 21). The processing is imperfect, however, since the receiver normally cannot tell if differences between adjacent lines of an image frame comprised of two interlaced fields are due to motion, or to vertical details. When still images with significant vertical detail are processed using algorithms optimized for motion images, such as those based on median filtering, the IDTV processing can sometimes increase the interline flicker instead of eliminating it. However, for still video graphics or Photo CD still images, the source could tell the receiver when repeated frames occur, using vertical interval codes.

All new receivers will soon include circuitry to decode the line 21 closed-captioning data. This same circuitry could also be used to decode origination-source ID data placed in the vertical interval, (Fig. 22). The source-adaptive IDTV receiver can perform perfect progressive scan conversion, using the circuitry shown in Fig. 23. This circuit is identical to a standard interlace-to-progressive scan conversion circuit currently used in IDTV receivers, except for the multiplexer that follows the median filter. When repeat frame images are detected, the median filter used for the missing line interpolation of motion images is bypassed, since the values from the field store are identical to the values of the missing lines. Cross color and

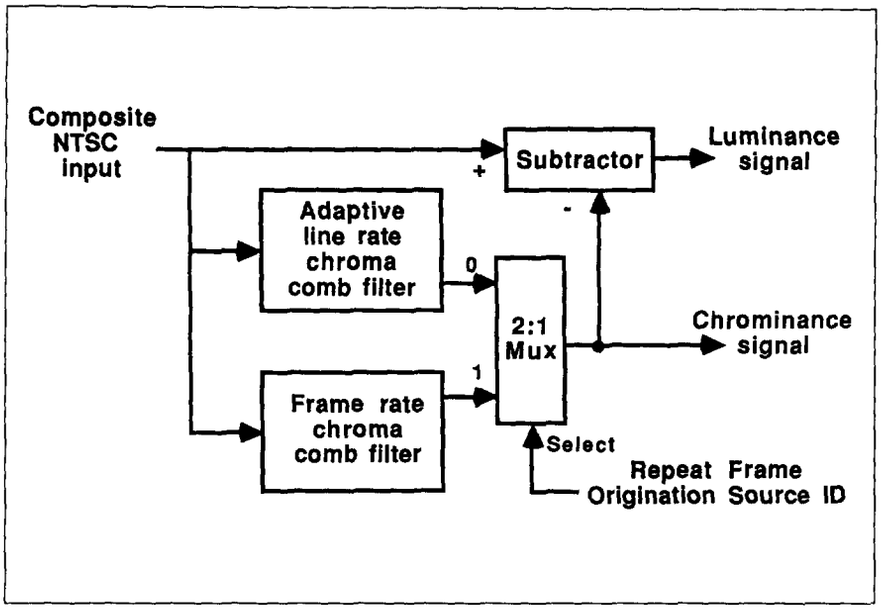


*Figure 24. Luminance/chrominance separation for repeat frames.*

dot crawl can be totally eliminated from repeat frame images using the circuitry shown in Fig. 24, since a frame-rate comb filter provides perfect chrominance separation for still images. Improved noise reduction for repeat frame images can be accomplished by using well-known IIR filtering techniques[19] and switching to a larger feedback coefficient when repeat frame images are detected.

For motion-picture film sources, the source ID would identify the real film frames. This enables perfect progressive scan conversion, using a full frame store in the receiver.[20,21] It also allows improved NTSC decoding, since every fifth video field is a repeated field from the same film frame, and thus contains no motion.[21] The aspect-ratio ID allows widescreen receivers to automatically switch to full-height mode for letterbox movies. Techniques based on recognizing real film frames following film-to-video conversion via 3:2 pulldown have also been used to provide improved NTSC-to-PAL conversion of film-originated programs,[22] and improved EDTV transmission of film images via the "Fukinuki hole."[23]

## Origination-Source ID Data

In order to make source-adaptive encoding more efficient to implement, origination-source ID data should be incorporated into the video signal during post-production. Key parameters include the frame rate, interlace or progressive scanning, repeated frames, real film frames, resolution level or active line count, aspect ratio, and color mode. In order to be useful, this data must be properly passed through all production stages and arrive at the receiver. It must incorporate adequate error protection, and should be compact and extensible to allow for future growth. Work on a number of related standards is going on within the SMPTE Working Group on Headers/Descriptors (P18.01), the SMPTE Ad Hoc Group on Video Index (P18.41), and the EIA TV Data Systems standards group. These groups are the logical place to consider original-source ID standards

## Conclusion

North America will soon be making a decision on adopting an HDTV transmission standard that will take it into the 21st century. The prospects of an all-digital system, with its ability to deliver high-quality television to the home, hold great promise. Such a system must use the spectrum as efficiently as possible in order to maximize the image quality. To that end, source-adaptive encoding is a simple yet tremendously important idea that should be an integral part of any HDTV system is adopted. Source-adaptive encoding can be incorporated into any of the digital HDTV systems scheduled to be tested by the ATTC and can also be used in IDTV receivers. For this to happen, the required source-adaptive parameters and the origination-source ID format must be standardized.

## References


1. P. Monta and J. Lim, "Source Adaptive Processing for ATV System Design," presented at 132nd SMPTE Technical Conference, New York, Oct. 1990.
2. W. F. Schreiber et al., "Channel-Compatible 6-MHz HDTV Distribution Systems," *SMPTE J.*, *98*:5-13, Jan. 1989.
3. Proc. *IRE*, Second Color Television Issue, Jan. 1954, Institute of Radio Engineers, New York.
4. E. J. Berkhoff et al., "Applications of Picture Memories in Television Receivers," *IEEE Trans. on Consumer Electronics*, *CE-29*:251-258, Aug. 1983.
5. E. Dubois, "The Sampling and Reconstruction of Time Varying Imagery with Application in Video Systems," *Proc. IEEE*, 73: 501-522, April 1985.
6. S. C. Hsu, "The Kell Factor: Past and Present," *SMPTE J.*, *95*:206-214, Feb. 1986.
7. M. A. Isnardi, "Multidimensional Interpretation of NTSC Encoding and Decoding," *IEEE Trans. on Consumer Electronics*, *34*:179-193, Feb. 1988.
8. C. B. Hunt et al., "High-Resolution Electronic Intermediate System for Motion-Picture Film," *SMPTE J.*, *100*:156-161, Mar. 1991.
9. L. E. DeMarsh, et al., "Scanning Requirements for Motion-Picture Post-Production," *SMPTE J.*, *94*:921-924, Sept. 1985.
10. M. Kriss et al., "Critical Technologies for Electronic Still Imaging Systems," *Applications of Electronic Imaging*," SPIE, 1082:157-184, 1989.
11. L. J. Thorpe and T. Hanabusa, "If Progressive Scanning is So Good, How Bad is Interlace?" *SMPTE J.*, *99*:972-986, Dec. 1990.
12. G. R. Hubbard, "The Photo CD System: An Overview for Consumer and Photofinishing Applications," *IEEE Intl. Conf. on Consumer Electronics Digest of Technical Papers*, pp. 316-317, June 1991.
13. "Digicipher HDTV System Description," General Instrument Corp., July 26, 1991.
17. T. Liu and W. F. Wedam, "Hardware Implementation and Cost of Decoders for Digital HDTV," *IEEE Trans. on Consumer Electronics*, *37*:331-336, Aug. 1991.
18. C. A. Poynton, "A Tutorial on Magic Numbers for High Definition Electronic Production," presented at 132nd SMPTE Technical Conference, New York, Oct. 1990.
19. R. H. McMann,et al., "A Digital Noise Reducer for Encoded NTSC Signals," *SMPTE J.*, *87*:129-133, March 1978.
20. Y. C. Faroudja, "Film-To-Video Converter With Scan Line Doubling," U.S. Patent 4,876,596, Oct. 24, 1989.
21. E. A. Krause, "Progressive Scan Display of Video Derived from Film," U.S. Patent 4,881,125, Nov. 14, 1989.
22. D. A. Jaqua, "High Resolution Translation of Images," U.S. Patent 4,998,167, Mar. 5, 1991.
23. M. Kageyama et al., "New Multiplex/Separation Schemes for Telecine Images," *IEEE Trans. on Consumer Electronics*, *37*:291-295, Aug. 1991.

# A 1-Megapixel, Progressive-Scan Image Sensor with Antiblooming Control and Lag-Free Operation

Eric G. Stevens, *Member, IEEE*, Bruce C. Burkey, *Senior Member, IEEE*, David N. Nichols, *Member, IEEE*, Ying S. Yee, David L. Losee, *Member, IEEE*, Teh-Hsuang Lee, *Member, IEEE*, Timothy J. Tredwell, *Senior Member, IEEE*, and Rajindar P. Khosla, *Fellow, IEEE*

***Abstract*—A 1024 × 1024 pixel, interline charge-coupled device (IL CCD) image sensor has been developed that incorporates antiblooming and electronic exposure control while eliminating lag and obtaining a high responsivity. The novel features of this device include a noninterlaced, or progressive-scan architecture and dual-horizontal registers that can be used to clock out the image area by one or two lines at a time. These features make it well suited for applications demanding high-resolution-image capture from a single, high-speed scan.**

## I. Introduction

ALTHOUGH several megapixel image sensors have been developed recently to satisfy high-definition television's (HDTV) resolution requirements [1]–[3], they are not ideally suited for high-resolution, robotic vision and other electronic camera applications. Their interlaced architecture results in a 50% loss of resolution in systems that must capture an image in a single scan. Also, the problem of eliminating image lag, while providing antiblooming and electronic-exposure control needs further investigation.

Antiblooming and electronic exposure control are two very important and desirable features of a solid-state image sensor for both consumer and industrial applications. Although antiblooming is an absolute necessity in uncontrolled lighting situations, it is also often required in environments with controlled illumination. In robotic vision applications, for example, specular reflections from sharp, metallic surfaces may cause blooming, which can degrade or completely destroy the image's integrity. It is also highly desirable to incorporate electronic shuttering in an electronic camera, from a long-term reliability standpoint, so that its mechanical counterpart can be eliminated.

Although it is very important to provide these features, other performance aspects of the device, such as low lag, low smear, and high responsivity, must not be compromised. These two features have been incorporated in a 1.0-Mpixel IL CCD image sensor with a noninterlaced scan whose pixel structure also provides low smear, no image lag, and high responsivity. The device's pixels measure 9 × 9 $\mu m^2$, and the resulting chip size is approximately 10 × 10 $mm^2$.

Manuscript received August 10, 1990; revised November 19, 1990.
The authors are with Eastman Kodak Company, Microelectronic Technology Division, Rochester, NY 14650-2008.
IEEE Log Number 9143226.

## II. Basic Device Architecture and Design

A functional block diagram of the device is shown in Fig. 1, and the pixel architecture is shown in Fig. 2. The device is designed using an IL, two-phase (2Φ), buried-channel CCD process. Double polysilicon and metallization layers are employed. The flat p-well and overlaying n-type layer, as shown in Fig. 2, are formed by implanting boron and then phosphorus into the 30-Ω · cm n-epitaxial layer. This light p-well implant is also used as the p tub for the horizontal CCD's (HCCD). The n well, however, is only used in the image area. To form the vertical CCD's (VCCD) and transfer gates, the n well is compensated for underneath these areas by a heavier boron, p-stripe implant. After the VCCD's are formed using a shallow arsenic buried-channel implant, the top $p^+$ layer within the photodetectors is implanted with a shallow boron implant, in a self-aligned manner. An additional phosphorus implant is added to the detectors just prior to this implant to adjust their empty-channel potential.

These resulting $p^+$-n-p-$n^-$ photodetector elements operate in a fully depleted mode. That is, the n layer sandwiched between the $p^+$ and uniform p layers is fully depleted. Therefore, charge from the photodiodes can be completely transferred to the VCCD thereby eliminating image lag [3] as seen with conventional n-p photodiodes [4], [5] and overlaying amorphous silicon photoconductors [1]. The uniform, p-type layer eliminates barriers between the center of the photodiode and transfer gate, which can also cause lag, as seen with other structures [2], and as reported here. The image area consists of a total of 1024 × 1024 pixels with 10 dark-reference pixels at the beginning of each line. Use of 2Φ VCCD's makes it possible to obtain a noninterlaced scan with only 9 × 9 $\mu m^2$ pixels. The 1.2-$\mu$m channel stops and a 3.2-$\mu$m-wide 2Φ VCCD result in a photodiode-to-pixel-area ratio of 29% (the photodiode's optical aperture was designed at 20%). The 3.2-$\mu$m-wide 2Φ VCCD has 1.2-$\mu$m-long barrier regions and 3.3-$\mu$m-long storage regions, resulting in a measured charge capacity of 50 000 $e^-$. The dynamic range of the VCCD's is greater than 60 dB. The charge capacity of the photodiode depends on how much anti-

0018-9383/91/0500-0981$01.00 © 1991 IEEE

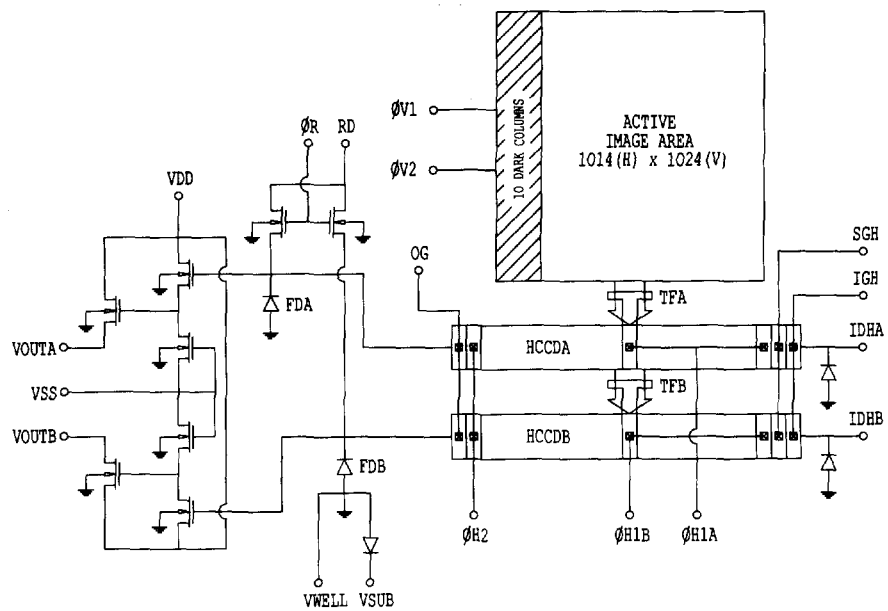


Fig. 1. Functional block diagram of the device.

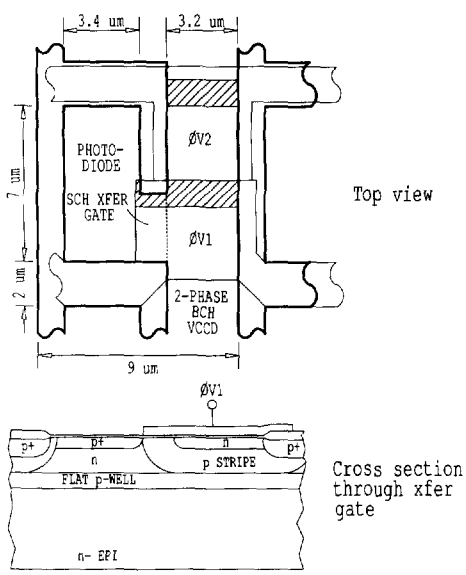


Fig. 2. Planar and cross-sectional views of the pixel.

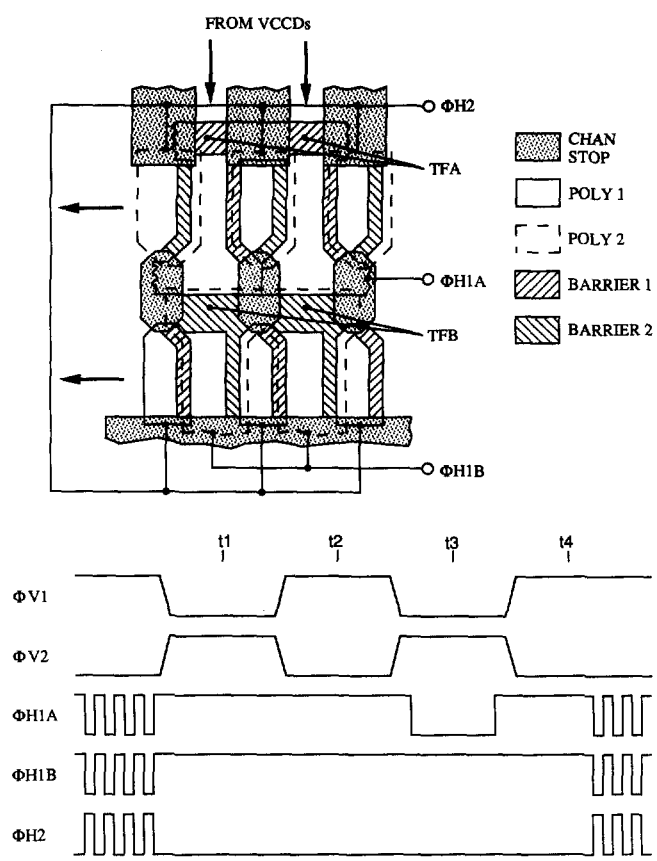


Fig. 3. Planar view and timing of *A*-to-*B* HCCD transfer.

blooming protection is required, and is adjusted by the bias applied to the substrate.

## III. Horizontal CCD's

The dual 2Φ HCCD design can be used for parallel readout of two complete lines of signal charge at data rates up to 30 frames/s. This high-speed HCCD readout ($f_{HCCD}$ = 20 MHz) is accomplished by forming these HCCD's in the same light p-well regions used to create the flat p layer in the image area as mentioned above. This results in large fringing fields that aid in charge transport. Also, since each HCCD has enough pixels to contain a full line of information from the image area, a single-channel readout mode can also be used if desired. A separate transfer gate between the HCCD registers as used in other designs [6], [7], has been eliminated. Therefore, only three clocks are required to operate both HCCD's. The layout of this region and timing for *A*-to-*B* register transfer are shown in Fig. 3. The layout of this HCCD transfer region was carefully constructed to eliminate transfer noise that could be caused by barriers introduced by narrow-channel effects. This was accomplished without the

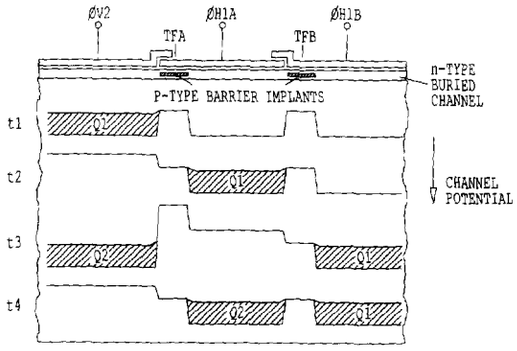


Fig. 4. Operation of $A$-to-$B$ HCCD transfer.

need for a third level of polysilicon as used by others [6], [7], thereby simplifying the process. The cross section shown in Fig. 4 illustrates how the $A$-to-$B$ register transfer is achieved. At time $t1$, $\Phi V2$ is high and holds charge packet $Q1$ while $\Phi H1A$ and $\Phi H1B$ are also held high ready for transfer. Then, at time $t2$, $\Phi V2$ goes low, transferring charge packet $Q1$ into $\Phi H1A$. Next at $t3$, $\Phi V2$ goes high again to receive charge packet $Q2$ from the next line of the image area. Also at this time, $t3$, $\Phi H1A$ goes low thereby transferring $Q1$ into the $B$ register's $\Phi H1B$. Then at $t4$, $\Phi H1A$ goes high and $\Phi V2$ goes low to transfer charge packet $Q2$ into the $A$ register's $\Phi H1A$. Subsequently, $\Phi H1A$ and $\Phi H1B$ are clocked in unison to read out these two lines. Since they are clocked in unison, the barrier region, TFB, at the leading edge of $\Phi H1B$ maintains the separation of charge packets $Q1$ and $Q2$. Single register readout is accomplished by starting the HCCD readout between times $t2$ and $t3$, and by leaving $\Phi V1$ and $\Phi V2$ in their high and low states, respectively.

The charge capacity of each HCCD is twice that of the VCCD's so that $2 \times 1$ charge aggregation can be performed if desirable in either the dual- or single-line readout mode of operation.

## IV. Output Structures

The output structure consists of two independent, floating diffusion amplifiers, one for each HCCD. An optimized, two-stage, source-follower configuration is used for each of the output buffers for low-noise, high-speed performance while minimizing signal attenuation. Reducing signal attenuation is important in reducing the off-chip system noise as it is referred back to the floating diffusion by one over the gain, i.e., by $1/A_v$. The first-stage load transistor's gate is zero biased to reduce the pin out and more importantly, to eliminate the noise introduced from this node. The second-stage current loads are off chip to reduce on-chip power dissipation.

This electrometer's design incorporates buried-channel, LDD-like FET's for the reset gate, output gate, and source-follower transistors to increase its voltage responsivity and reduce noise as previously reported [8]. The LDD/LDS reset FET has the same channel implant used for the storage regions of the CCD's. The LDD output

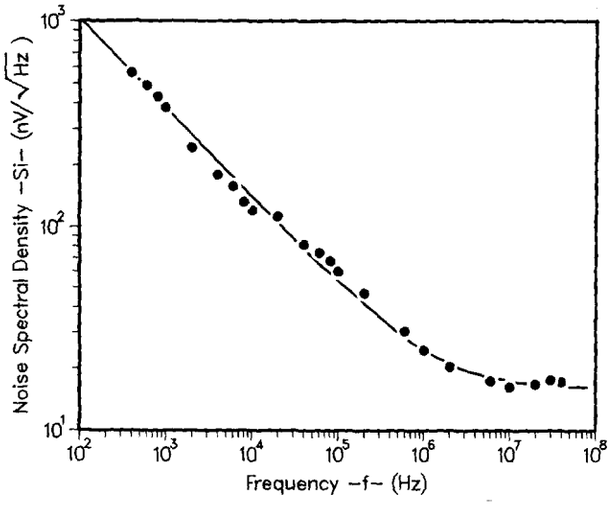


Fig. 5. Measured output-buffer noise spectral density. A fit to the measured data (shown as the single points) is

$$S_t^2 = \frac{58(10^{-12})}{f^{0.87}} + 2.56(10^{-16})\,(\mathrm{V}^2/\mathrm{Hz}).$$

gate and source-follower FET's receive the CCD transfer-, or barrier-region implants. In addition, the source-follower's FET's are formed in light p-well, and heavy p-stripe-implanted areas. Although this reduces the amplifier's gain somewhat due to the increased body effect, it is necessary to prevent vertical punchthrough to the substrate.

The measured input-referred voltage responsivity of these electrometers is over 14 $\mu$V/e$^-$. The thermal-noise voltage of these buried-channel (BCH) FET's was found to be comparable to that of surface-channel (SCH) FET's since their transconductances ($g_m$) were equal. This is because the reduced gate-to-channel capacitance of these BCH FET's is compensated by their higher channel mobility. Hence, using the BCH FET's results in a lower level of $1/f$ and thermal input-referred noise in terms of electrons rms. The input-referred noise spectral density of these amplifiers is shown in Fig. 5. Without correlated double sampling, but excluding the reset $kTC$ noise, the input-referred noise of these amplifiers is only 10 e$^-$ rms.

The low-input capacitance of these BCH LDD FET's also increases the bandwidth of the two-stage buffers for high-speed operation. To further enhance the bandwidth of these amplifiers, the source-follower's drive FET's have conventionally aligned n$^+$-source implants to reduce the series resistance in the source ($R_S$) as shown in Fig. 6. Hence the source-follower's output resistance ($R_{\mathrm{OUT}}$) given by

$$R_{\mathrm{OUT}} \approx A_v(1/g_m + R_S) \tag{1}$$

is reduced. Although this self-aligned implant also increases the gate-to-source overlap capacitance ($C_{GSO}$), its affect on the overall input capacitance ($C_{\mathrm{IN}}$) of the source-follower configuration is negligible since this term adds very little to the total gate-to-source capacitance ($C_{GS}$). Also, $C_{GS}$ is multiplied by the factor $(1 - A_v)$ due to the

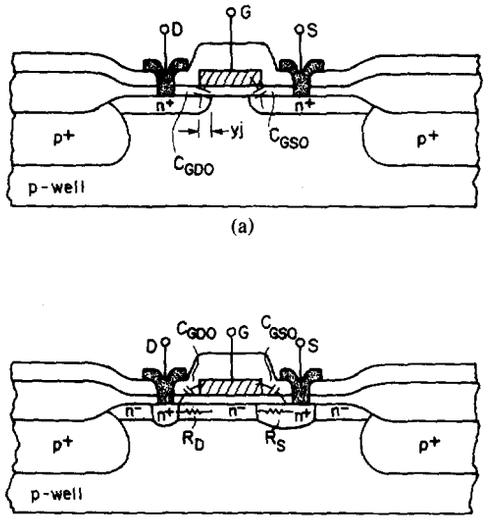


Fig. 6. Cross-sectional view of output amplifier's buried-channel, LDD drive transistors with self-aligned source implants. (a) Conventional surface-channel MOSFET with self-aligned-to-gate $n^+$ source and drains. (b) Buried-channel LDD MOSFET with self-aligned-to-gate $n^+$ source.

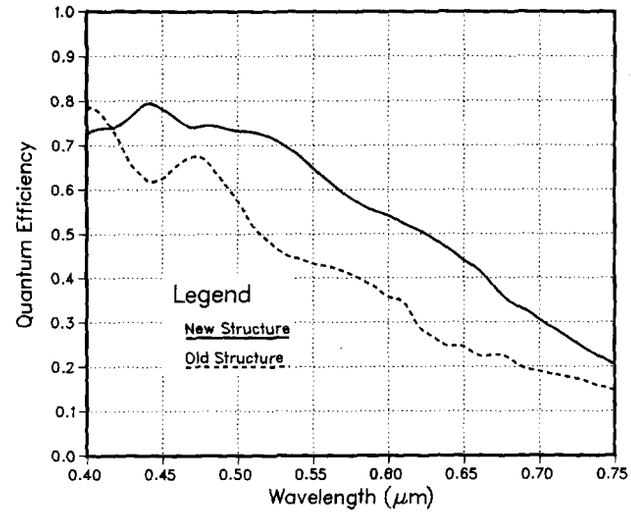


Fig. 7. Measured quantum efficiency of old and new VOD structures normalized for a 100% fill factor.

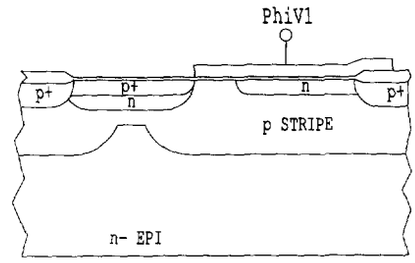


Fig. 8. Cross-sectional view of an older VOD structure design [9].

Miller effect which further reduces the effect of $C_{GSO}$ on $C_{IN}$ as given by

$$C_{IN} \approx (1 - A_v)\,[\tfrac{2}{3}\,WL(C'_{OX})_{eff} + WC'_{GSO}] + C_{GB} + WC'_{GDO}. \quad (2)$$

Measurement of the two-stage source-follower's frequency response shows that the −3-dB bandwidth of these buffers is over 60 MHz with a 10-pF load. This is sufficient for HCCD operation at speeds up to 20 MHz.

## V. Antiblooming and Photoresponse

An antiblooming or overflow barrier is formed beneath the photodiodes [9] in the thin p-type layer that lies on top of the n-type epitaxial layer as shown in Fig. 2. By creating this overflow point deep within the silicon, the detector's quantum efficiency ($\eta$) is increased since

$$\eta(\lambda) \approx T(\lambda)[1 - \exp(-\alpha(\lambda)x_o)] \quad (3)$$

where $T(\lambda)$ is the transmittance of the detector's overlayers, $\alpha(\lambda)$ is the absorption coefficient of silicon, and $x_o$ is the distance of this overflow point from the $Si$-$SiO_2$ interface. Since the absorption coefficient of silicon decreases for the longer wavelengths in the visible spectrum, the quantum efficiency is reduced in this region. This is because the carriers generated below the overflow point will be lost into the n-type substrate. Fig. 7 shows the measured quantum efficiency versus wavelength of this deep, uniform well structure compared to that of another device structure shown in Fig. 8 with a laterally diffused p-well VOD structure [9]. This VOD structure is seen to have a much shallower overflow point resulting in a lower quantum efficiency at longer wavelengths. For white light when integrated over a wavelength band of $400 < \lambda < 700$ nm, and using a fill factor of 20%, the new pixel structure's responsivity is determined to be 290 $ke^-/\mu J/cm^2$, or roughly 50 $nA/\mu W$ for the entire chip. This is over 50% higher than that of the laterally diffused p-well structure. In addition to a deeper overflow point, the flat p-well structure of this device results in a larger effective area of the photodiode. Measurements on devices with the laterally diffused p-well structure show that the center region of the photodiode is most sensitive to light. This can also be seen from electrostatic modeling of the structures. For devices with the laterally diffused p-well structure, most of the carriers generated near the edges of the photodiode are swept into the substrate since the overflow point is much shallower there. The depth of the overflow point for the new device with the flat p-well structure is much more uniform over the entire photodiode region. That is, the new structure has a much larger collection volume than that of the old type VOD structure.

Microlenticular arrays [10] have been built on these devices as outlined by Weiss [11], [12]. These anamorphic, or pillow-shaped lenses effectively increase the fill factor to over 60%. This increases the sensitivity of the device to over 150 $nA/\mu W$. Fig. 9 shows the measured quantum efficiency of a device with and without these lenses. From this figure, it can be seen that the average gain of the lens is over 3.0. Also, the gain is seen to be slightly less at shorter wavelengths due to some transmission loss within the lens-forming material.

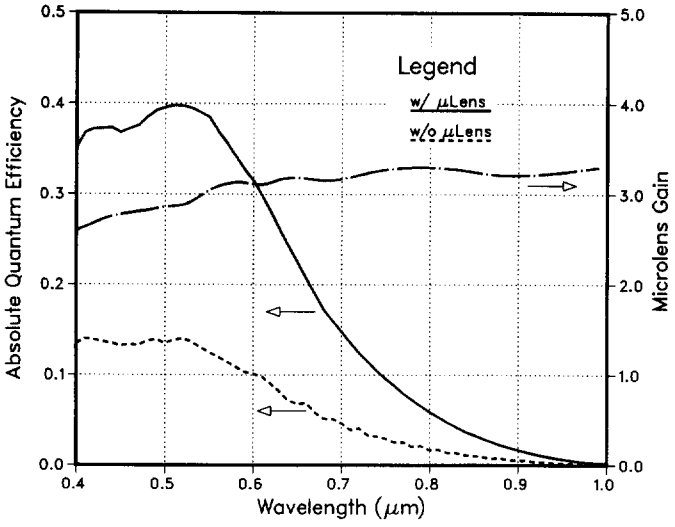


Fig. 9. Measured quantum efficiency of device with and with out microlens.

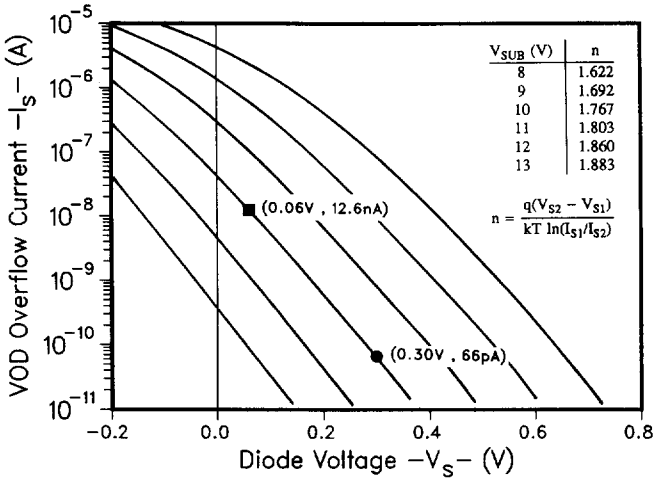


Fig. 10. Measured VOD nonideality factor versus substrate bias; 2-D modeling results in a nonideality factor of 2.0.

The photoresponse nonuniformity of a device with a lens array was measured and compared to that of the same device after removing the array. These measurements indicate that the gain uniformity of the lens array is at least less than that of the detector array itself.

Other important performance considerations that are affected by the antiblooming structure such as photoresponse linearity, dynamic range, and antiblooming protection can be shown to be directly related to this structure's nonideality factor $n$ and that a small value for this parameter is desirable [13]. The measured nonideality factor of this structure, as shown in Fig. 10, was found to be about $n = 1.8$ at a substrate voltage of $V_{SUB} = 10$ V. This compares favorably with other VOD pixel structures we have reported in the past [14], and is in good agreement with the modeling results of $n = 2.0$ at $V_{SUB} = 10$ V. Fig. 11 shows the measured photoresponse of this device from which it can be seen that this VOD structure exhibits a sharp turn-on. There is a tradeoff between the antiblooming protection provided and charge capacity of the photodiode [13]. By increasing the substrate bias the diode's capacity is decreased, and antiblooming protection increases.

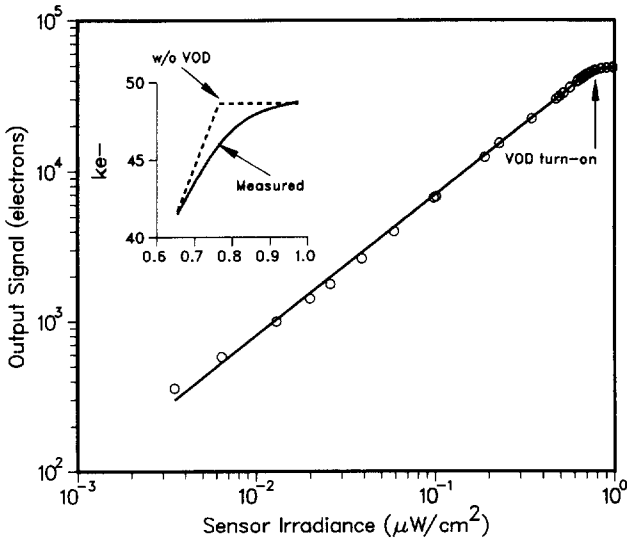


Fig. 11. Sensor's measured photoresponse linearity. The photoresponse nonlinearity at the knee is approximately 5%.

## VI. Image Lag and Smear

As can be seen in Fig. 2, the VCCD's are formed in a heavy, p-well stripe. This structure reduces smear by forming an electrostatic barrier between the detectors and VCCD's. The junction formed by the uniform, flat p-layer and n-type epitaxial layer also reduces smear by the same mechanism. In addition to reducing smear, the heavy p-well stripe serves to reduce well bounce problems (viz., image shading) and provide good VOD control. The smear of this device has been measured at $\approx 0.1\%$ with 100 lines (10% of the total image height) illuminated. This smear level is primarily due to light piping underneath the VCCD's aluminum light shields. This was further improved by reducing the dielectric thickness underneath these light shields using a refractory metal process [15]. In this case, a smear signal of only 0.02% has been measured.

As previously mentioned, the detector elements of this device are capable of operating in a fully depleted mode, thereby eliminating lag [3] and photodiode reset, or $kTC_{PD}$ noise. However, to completely deplete the n layer it is necessary to eliminate any potential barriers that may exist between the photodiode storage element and the photodiode-to-VCCD transfer gate. These barriers may be introduced in this structure if the heavy p-well stripe that is formed under the VCCD's diffuses laterally into the photodiode area. Therefore, process modeling and device simulation are required to eliminate these barriers by careful positioning of the well stripe's mask edge. These barriers may also be caused in part by the $p^+$ and n-type diode implants [16]. Fig. 12 shows the measured first-field decay lag as a percentage of full well versus the photodiode-to-VCCD barrier height. As can be seen from this figure, lag-free operation is obtained as the barrier height goes to

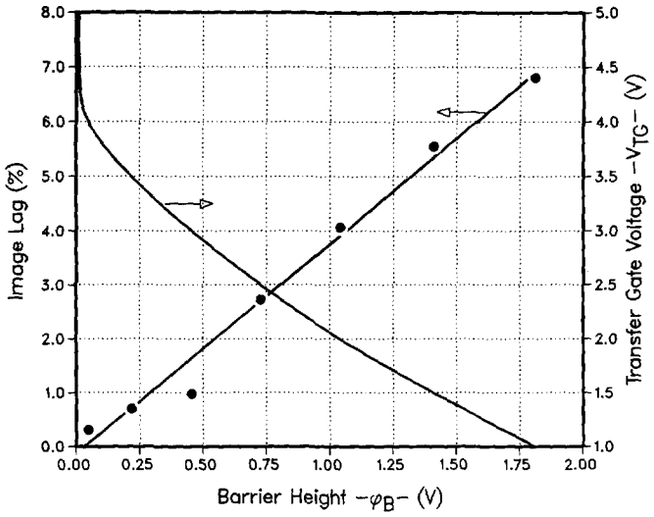


Fig. 12. Measured image lag as a percent of $V_{SAT}$ versus photodiode-to-VCCD barrier height.

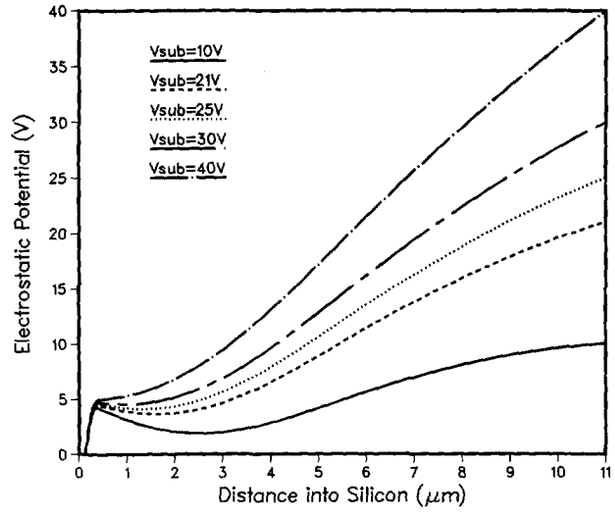


Fig. 13. Electrostatic potential simulations through middle of photodiode at various substrate potentials.

zero. The barrier height versus transfer-gate voltage shown in this figure was measured on a specially designed test structure. From this test structure, the potential of a fully depleted diode was measured at 3.2 V. It was also determined that a transfer-gate voltage of 3.0 V was required for the channel potential of this region to reach the empty-diode potential of 3.2 V. That is, a gate voltage of 3.0 V would be required to read out the photodiode in the absence of any barriers. Therefore, it can be seen from Fig. 12 that only about 1.5 V of overdrive on the transfer gate is required to substantially minimize any barriers and eliminate lag for this particular device.

## VII. Electronic Exposure Control

Electronic exposure control is employed by pulsing the n-type substrate to a sufficiently large voltage so as to pull down the overflow barrer via two-dimensional effects, as illustrated in Fig. 13. This will cause any charge in the photodiode to be swept out into the substrate, and hence the detector is reset to the empty diode potential. After this point, the substrate potential is returned to its normal level, and charge integration can begin. Fig. 14 shows the measured charge capacity as a percent of full-well versus substrate bias $V_{SUB}$ for two different n-well implant doses. Note that the heavier n-well dose results in a reduction in the substrate bias required to pull down the barrier to the substrate. This is because this barrier height is reduced at the higher dose.

This type of electronic-shuttering mode can be achieved since a complete charge transfer is possible from the $p^+$-n-p-$^-$ VOD detector structure. Devices with a conventional $n^+$-p-$n^-$ VOD structure cannot be electronically shuttered in this manner since the reset potential of the photodiode would differ between reset into the substrate and reset through the transfer gate, resulting in a large amount of pattern noise. Shutter speeds of 1/2000 of a second have been achieved using this method.

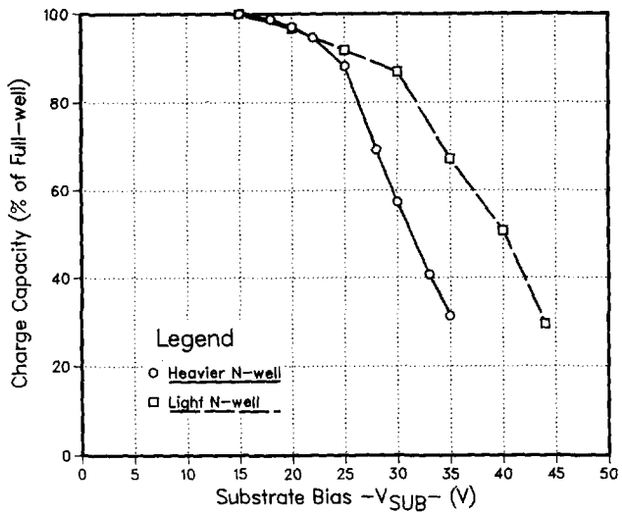


Fig. 14. Measured charge capacity versus substrate bias.

## VIII. Image Quality

Figs. 15 and 16 show reproductions of a high-definition television resolution chart taken by the sensor. Fig. 16 is a magnified portion of the center region of Fig. 15. Note that no blooming is noticed around the shiny, coaxial cable connector placed in the scene as would typically be seen for a device without an antiblooming structure. The low level of crosstalk afforded by the p-well VOD structure not only reduces smear, but enhances the resolution, or MTF, of the device as well. We have also observed that the use of the microlens arrays further improves resolution by cutting crosstalk, and helps to reduce aliasing by improving the fill factor. The dark-current noise for these devices is very low. Although these devices typically have photodiode dark-current densities of about 100 pA/cm$^2$ at 40°C, we have fabricated devices with values as low as 50 pA/cm$^2$ at this chip temperature. (The VCCD dark current can be reduced to similar levels or lower, by running the device in the accumulation mode

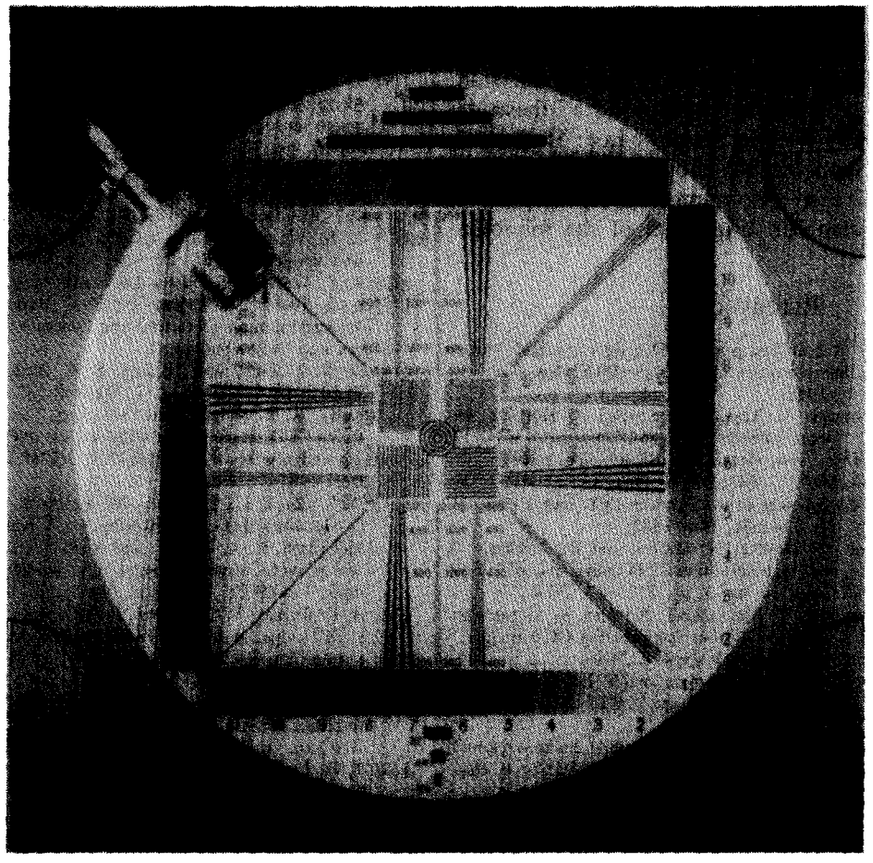

Fig. 15. Reproduced high-definition television resolution chart.

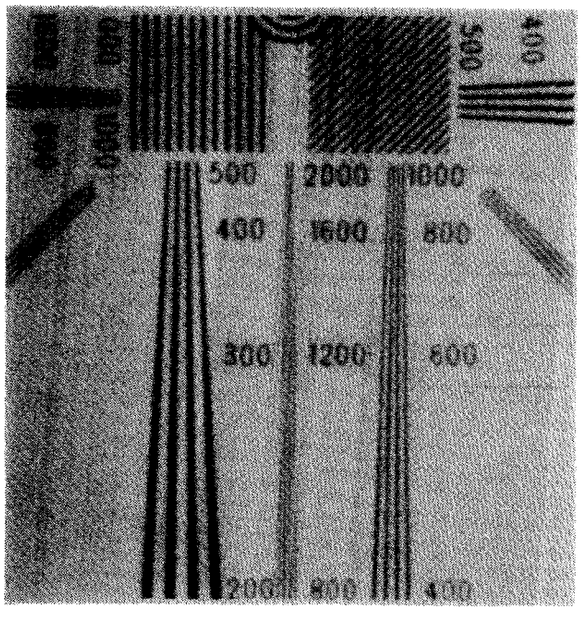


Fig. 16. Enlarged portion of Fig. 15 to show detail.

[17], [18].) This results in excellent image quality since when operating at 30 frames/s the total dark noise is dominated by the on-chip amplifier noise and other system noise components.

TABLE I
SENSOR PERFORMANCE SUMMARY

| Parameter | Value | Comments |
|---|---|---|
| Image area | 1020 × 1024 pixels | noninterlaced, including dark reference |
| Pixel size | $9 \times 9\ \mu m^2$ | |
| Charge capacity | 50 000 $e^-$ | VCCD's |
| Max dynamic range | >60 dB | VCCD's |
| Sensitivity | 870 $ke^-/\mu J/cm^2$ | w/$\mu$lens; $400 < \lambda < 700$ nm |
| Charge-to-voltage conversion | $>14\ \mu V/e^-$ | input referred |
| Image smear | 0.02% | 10% image height illuminated |
| Image lag | none | |
| Max data rate | $>30(10^6)$ pixels/s | 30 frames/s; $f_{HCCD} = 20$ MHz |

## IX. CONCLUSIONS

The incorporation of an antiblooming structure and electronic-exposure control into a 1-Mpixel IL CCD image sensor has been achieved without sacrificing other important device characteristics such as lag, smear, photoresponse linearity, and sensitivity. The progressive-scan architecture of this device offers the same resolution in an electronic-camera application as that of a 2-million element, interlaced device. Table I gives a summary of the performance characteristics of the device.

## Acknowledgment

The authors wish to thank the members of the processing labs of the Microelectronics Technology Division, Eastman Kodak Company, for fabrication of these devices. They especially wish to thank P. Lee, M. Parker, and Y.-R. Lee for supplying the photographs and some of the measured data. They also appreciate the help of A. Weiss and P. Whalen for fabrication of the microlenticular arrays.

## References

[1] S. Manabe *et al.*, "A 2-million pixel CCD imager overlaid with an amorphous silicon photoconversion layer," in *ISSCC Dig. Tech. Papers*, pp. 50-51, Feb. 1988.

[2] T. Nobusada, M. Azuma, H. Toyoda, T. Kuroda, K. Horii, T. Otsuki, and G. Kano, "Frame interline transfer CCD sensor for HDTV camera," in *ISCC Dig. Tech. Papers*, pp. 88-89, Feb. 1989.

[3] N. Teranishi, A. Kohono, Y. Ishihara, E. Oda, and K. Arai, "No image lag photodiode structure in the interline CCD image sensor," in *IEDM Tech. Dig.*, pp. 324-327, Dec. 1982.

[4] E. Oda, K. Nagano, T. Tanaka, N. Mutoh, and K. Orihara, "A 1920(H) × 1035(V) pixel high definition CCD image sensor," *IEEE J. Solid-State Circuits*, vol. 24, no. 3, pp. 711-717, 1989.

[5] T. Kuroda, T. Kuriyama, Y. Matsuda, T. Kozono, S. Matsumoto, Y. Hiroshima, and K. Horii, "A smear-suppressing CCD imager," in *ISSCC Dig. Tech. Papers*, pp. 94-95, Feb. 1986.

[6] E. Oda, K. Orihara, T. Tanaka, T. Kamata, and Y. Ishihara, "1/2-in 768(H) × 492(V) pixel CCD image sensor," *IEEE Trans. Electron Devices*, vol. 36, no. 1, pp. 46-53, 1989.

[7] K. Orihara and E. Oda, "New technologies in dual channel read-out registers for high density CCD image sensor," in *IEDM Tech. Dig.*, pp. 365-368, Dec. 1986.

[8] E. G. Stevens, T.-H. Lee, D. N. Nichols, C. N. Anagnostopoulos, B. C. Burkey, W.-C. Chang, T. M. Kelly, R. P. Khosla, D. L. Losee, and T. J. Tredwell, "A 1.4 million element CCD image sensor," in *ISSCC Dig. Tech. Papers*, pp. 114-115, Feb. 1987.

[9] Y. Ishihara, E. Oda, H. Tanigawa, N. Teranishi, E-I. Takeuchi, I. Akiyama, K-I. Arai, M. Nishimura, and T. Kamata, "Interline CCD image sensor with an antiblooming structure," in *ISSCC Dig. Tech. Papers*, pp. 168-169, Feb. 1982.

[10] Y. Ishihara and K. Tanigaki, "A high photosensivity IL-CCD image sensor with monolithic resin lens array," in *IEDM Tech. Dig.*, pp. 497-500, Dec. 1983.

[11] A. K. Weiss and C. P. Brophy, "Microlenticular arrays for solid-state imagers," *J. Electrochem. Soc.*, vol. 133, no. 3, p. 110C, 1986.

[12] A. K. Weiss, U.S. Patent 4 694 185, Sept. 15, 1987.

[13] E. G. Stevens, Y-R. Lee, and B. C. Burkey, "The effects of smear on antiblooming protection and dynamic range of solid-state image sensors," to be published.

[14] D. N. Nichols, W-C. Chang, B. C. Burkey, E. G. Stevens, E. A. Trabka, D. L. Losee, T. J. Tredwell, C. V. Stancampiano, T. M. Kelly, R. P. Khosla, and T-H. Lee, "A 1.4 million element, full frame CCD image sensor with vertical overflow drain for antiblooming and low color crosstalk," in *IEDM Tech. Dig.*, pp. 120-123, Dec. 1987.

[15] D. L. Losee, J. C. Cassidy, M. Mehra, E. T. Nelson, B. C. Burkey, G. Geisbuesch, G. A. Hawkins, R. P. Khosla, J. P. Lavine, W. C. McColgin, E. A. Trabka, and A. K. Weiss, "A 1/3" format image sensor with refractory metal light shield for color video applications," in *ISSCC Dig. Tech. Papers*, pp. 90-91, Feb. 1989.

[16] B. C. Burkey, W-C. Chang, J. Littlehale, T-H. Lee, T. J. Tredwell, J. P. Lavine, and E. A. Trabka, "The pinned photodiode for an interline-transfer CCD image sensor," in *IEDM Tech. Dig.*, pp. 28-31, Dec. 1984.

[17] N. S. Saks, "A technique for suppressing dark current generated by interface states in buried channel CCD imagers," *IEEE Electron Device Lett.*, vol. EDL-1, no. 7, pp. 131-133, July 1980.

[18] T. H. Lee, W-C. Chang, W. A. Miller, G. R. Torok, K. Y. Wong, B. C. Burkey, and R. P. Khosla, "A four million pixel CCD image sensor," in *Proc. of SPIE*, vol. 1242, Feb. 1990.

# Single-Chip Color HDTV Image Sensor with Two Polysilicon Levels and with $WSi_x$ Lightshield Used for Strapping Vertical Gates

D. N. Nichols, C. V. Stancampiano, G. R. Torok, J. P. Lavine, E. G. Stevens, B. C. Burkey, T. H. Lee, J. Jech, M. R. Suchanski, E. A. Trabka, and R. P. Khosla

Eastman Kodak Company, Microelectronics Technology Division
Rochester, New York 14650-2008

## Abstract

A single-chip, color, high-definition television (HDTV) image sensor with only two polysilicon levels and $WSi_x$ strapping of the vertical CCD has been developed. The sensor has square pixels and a vertical-stripe color filter pattern for simplified image processing.

## Introduction

High-resolution, single-chip color image sensors operating at video frame rates are needed for several applications including high-definition television (HDTV), microscopy, and medical imaging. Because of increased pixel count and pixel readout rate, HDTV sensors have become increasingly complex. For example, three polysilicon levels are needed on full resolution interline (1), frame interline transfer (2), and frame transfer (3) HDTV sensors. This paper describes the architecture, operation, and characterization of an HDTV sensor with only two polysilicon levels, that uses the lightshield metal to speed up the vertical gates. A vertical-stripe color filter array enables the use of a more simplified image processing scheme than a previously reported (4) HDTV single-chip color sensor.

## Basic Device Architecture

The block diagram for the device is shown in Fig. 1. The interlaced, interline transfer sensor has 1920 (H) x 1080 (V) optically active, square pixels with a pixel size of 7.3 µm x 7.3 µm. The optically active area of 14.0 mm x 7.9 mm has a 16:9 aspect ratio compatible with a 1" optical format. This architecture is consistent with the "common image format" (CIF) (5), providing square pixels to simplify image processing for commercial and government applications. Fig. 2 shows the pixel architecture. The pixels consist of a "pinned" p+npn photodetector (6) for vertical blooming protection and no lag. The vertical CCD is constructed with a buried channel, two-phase design. The two-phase CCD enables the use of only one CCD gate per pixel. The barrier length for the vertical CCD is 1.2 µm, leaving 6.1 µm for the storage region. To maintain charge capacity with this small pixel, the isolation in the horizontal direction is defined with 1 µm lithography. The resultant VCCD charge capacity is 80,000 electrons.

## $WSi_x$ Lightshield and VCCD Strap

A 0.6-µm-thick $WSi_x$ film is used for lightshield (7) for several reasons. $WSi_x$ withstands the high temperature required for reflow of borophosphorsilicate glass (BPSG). Therefore, the $WSi_x$ lightshield can be placed very close to the vertical gate to reduce smear, and BPSG is reflowed over the lightshield to improve topography for metallization. Only

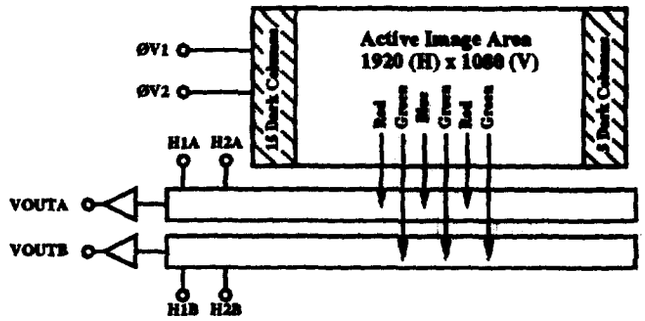


Fig. 1 Block diagram of the device.

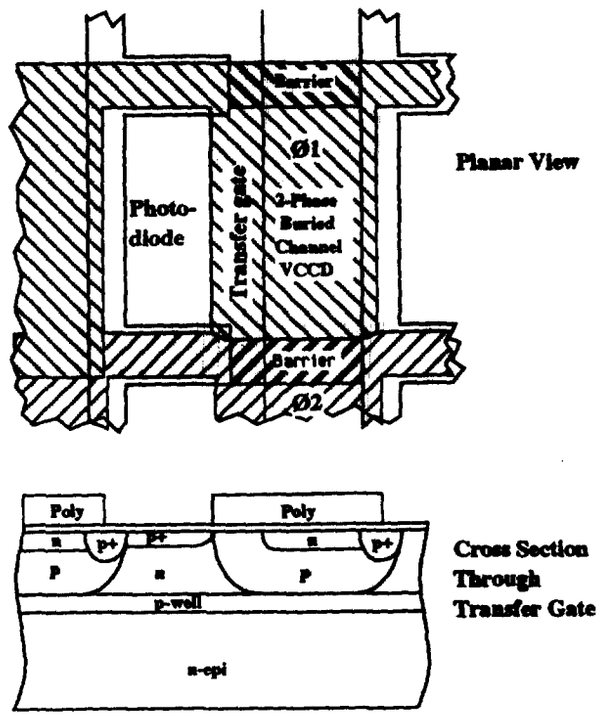


Fig. 2. Pixel architecture.



0-7803-0817-4/92 $3.00 © 1992 IEEE

a 250-nm oxide layer separates the polysilicon gate from the lightshield. The etched $WSi_x$ edge is less ragged than that of aluminum, resulting in less fixed pattern noise. $WSi_x$ is also less reflective than aluminum, further reducing smear. The low resistivity of refractory metals and their silicides provide excellent conductors to strap the VCCD gates (3,8). Contact holes (1.4 μm) between the vertical gates and the lightshield are used to speed up the VCCD. The silicide film is deposited with excess silicon, and no silicide spiking occurs into the gate. Therefore, unlike aluminum strapping (2) where an additional polysilicon layer is used to prevent local work function differences due to aluminum spiking, no additional polysilicon layer is needed. The n+ polysilicon to $WSi_x$ contact resistance through the hole is 30 ohms. The resultant RC time constant for vertical clocks is well below 1 μs. Fig. 3 shows a cross-sectional SEM of a pixel with the silicide lightshield and the contact to the vertical polysilicon gate.

Fig. 3. Cross-sectional SEM showing the $WSi_x$ contact to a polysilicon gate.

### Horizontal CCDs and Output Structures

The architecture of the dual HCCDs enables the readout of one horizontal line in two parallel CCDs, each capable of operating over 38 MHz. Therefore, data rates of up to 76.5 MHz, required for the CIF, can be obtained. The HCCD design is shown in Fig. 4, and the timing and charge transport are depicted in Fig. 5. For each line, charge from odd columns is transferred to an output using the A register, and charge from even columns is transferred to an output using the B register. Complete transfer of one line from the last vertical gate to the two HCCDs takes place during the horizontal retrace time, as follows. After one full line is transferred to the A register, all gates of the A register are simultaneously turned off, transferring charge in H1A to H1B, while maintaining the charge in H2A. The charge capacity of each gate in this two-phase CCD is designed (based on two-dimensional process and device modeling) to hold more than 100,000 electrons with the gate in accumulation, i.e, at its low level. Then H1B is turned off, transferring its charge to H2B. Charge transfer to the B register is performed through one phase of the A register without the use of a separate transfer gate. Therefore, this design simplifies the fabrication process, since a separate transfer gate often uses a third level of polysilicon (1,2). Careful three-dimensional device modeling based on two-dimensional process modeling was used to ensure that no potential pockets exist in the design. Monte Carlo modeling, along with the three-dimensional channel potential results, were used to evaluate the time for transfer of charge to the B register. Modeling results indicate complete transfer in less than 100 ns. Similar Monte Carlo modeling for transfer along the A register, from H1A to H2A, was done to ensure that no charge was trapped in the lower region of H1A. Channel potential contours and the simulation of the last electron's travel from the lower left corner of H1A to H2A is shown in Fig. 6. Results show that while the charge diffuses in the low field region of H1A for a short time, the time for traveling to H2A is much shorter than the horizontal clock period. Experimental results indicate complete charge transfer from the A to the B register in less than 2.2 μs, and very good charge transfer efficiency along the HCCD.

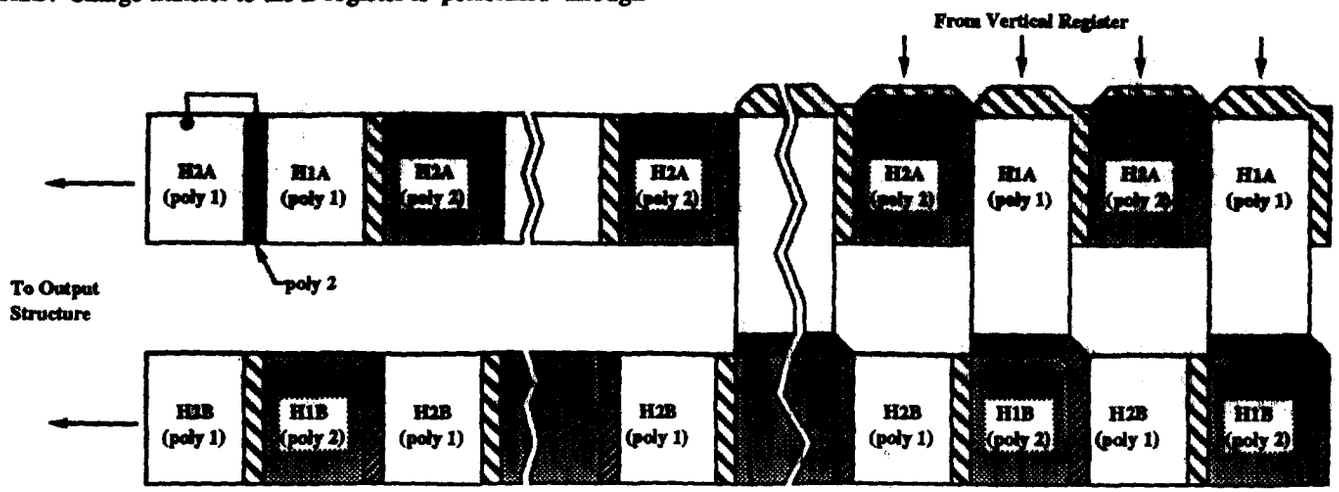


Fig. 4. Design for the dual HCCDs.

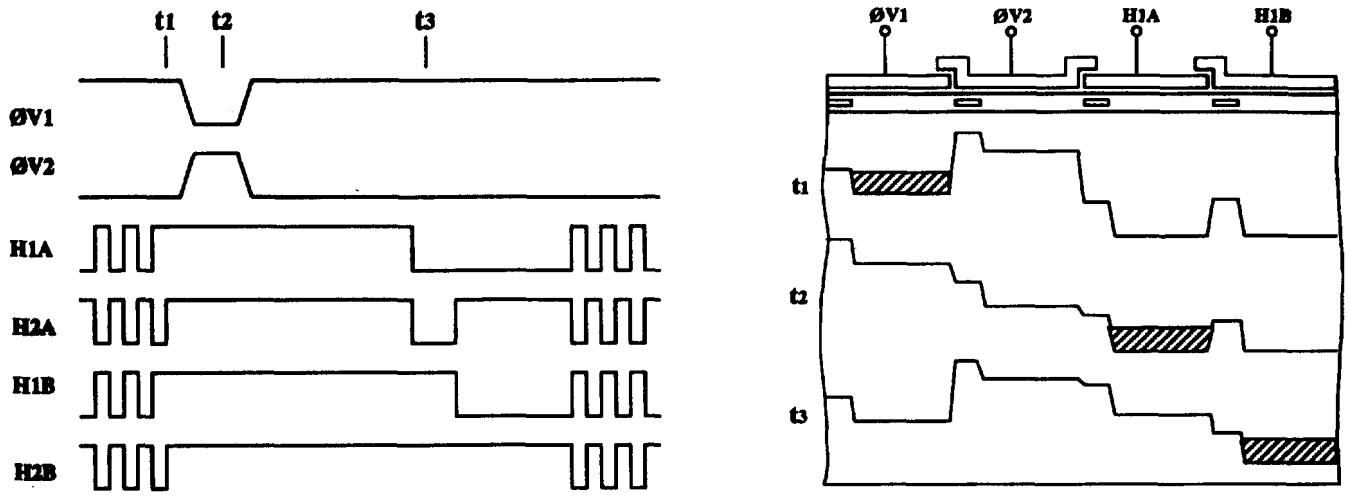


Fig. 5. Timing and operation of the A to B HCCD transfer.

A gate that combines a poly 1 storage region with a poly 2 barrier region is used on the A register near the output structure to switch the last gate from poly 2 to poly 1. This enables the two output gates to be formed of the same poly level so that the two output structures are better matched.

Two matched floating diffusion amplifiers (one for each HCCD) are used to sense the charge. Each sense amplifier embodies a separate three-stage, source-follower output buffer. These output structures use buried-channel, LDD FETs for the reset gate, output gate, and first-stage, source-follower transistors for higher responsivity and lower noise, similar to those reported in (6). The voltage responsivity of the output structure (including the three-stage source-follower) is 8 $\mu V/e^-$. The measured bandwidth of the source-followers is over 148 MHz with a 10 pF load.

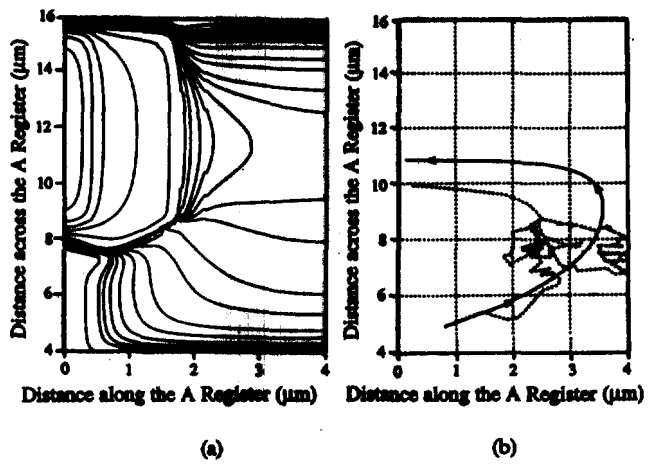


Fig. 6. Three-dimensional modeling result for transfer along the A register. (a) Contour plot of channel potential. (b) Single electron's path for drift only (solid line), and for drift and thermal diffusion (dotted line).

## Color Filter and Microlenticular Arrays

Red, green, and blue color filters are fabricated on the sensor to obtain full color information from a single chip. The vertical-stripe color filter array is designed so that all green information is transferred to the B register, and red and blue information is read out from the A register, as shown in Fig. 1. Color image processing is therefore simplified because color separation is easily performed. In addition, luminance and chrominance signals are sensed and buffered by separate output amplifiers to avoid amplifier gain mismatch problems. An integral microlenticular array is used to increase the sensitivity by a factor of 2.5.

## Imaging Characteristics

The measured photoresponse curve is shown Fig. 7. The sensor's output is linear with light level until the relatively sharp turn-on of the vertical overflow drain. Dynamic range for the sensor is 63 dB. The "pinned" photodetector incorporates a vertical overflow drain for blooming protection

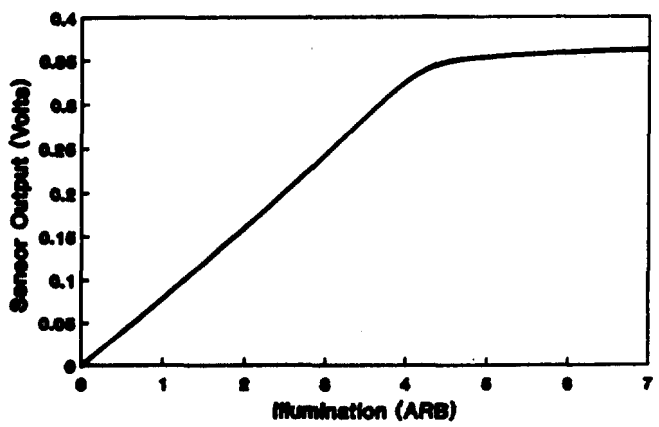


Fig. 7. Measured photoresponse for the sensor.

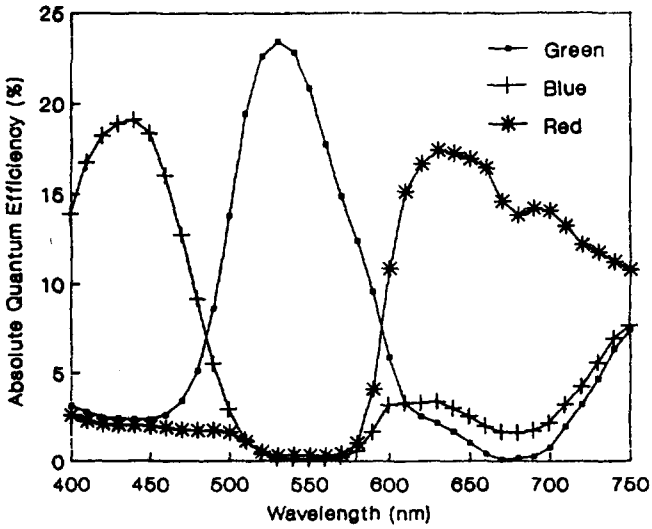


Fig. 8. Measured spectral response curves for the HDTV image sensor.

of at least 300 times the photodiode capacity. This photodetector structure also is lag-free with only a 1.5 V overdrive of the transfer gate (6). The silicide lightshield is quite effective at reducing the smear. Smear is only -77 dB for the color sensor. The spectral response curves are shown in Fig 8. Good sensitivity and color separation are obtained. Color images captured by the sensor at 30 frames/s show very good color rendition, indicating excellent transfer from the A to the B register, and along the HCCDs. An image of a black-and-white resolution target captured at 30 frames/s by the color sensor and displayed on a color HDTV monitor is shown in Fig. 9.

## Conclusions

A single-chip, color, 2-megapixel, interline-transfer HDTV sensor has been demonstrated. The sensor is designed with square pixels and a vertical-stripe color filter array to simplify signal processing. In addition, the sensor uses $WSi_x$ strapping of vertical clocks and dual HCCDs with only two polysilicon layers.

## Acknowledgements

The authors thank the Fabrication Department of the Microelectronics Technology Division for wafer processing, and Alfred O. Bitek and James Koudelka for systems work.

## References

(1) E. Oda, K. Nagano, T. Tanaka, N. Mutoh, and K. Orihara, "A 1920(H) x 1035(V) pixel high-definition CCD image sensor," IEEE J. Solid-State Circuits, vol. 24, pp.711-717, June 1989.

(2) M. Yamagishi, et al., "A 2 million pixel FIT-CCD image sensor for HDTV camera systems," IEEE Trans. Electron Devices, vol. 38, pp. 976-980, May 1991.

(3) A. Theuwissen, et al. "A 2.2 Mpixel FT-CCD imager, according to the Eureka HDTV-standard," IEDM Tech. Digest, pp.167-170, Dec. 1991.

(4) T. Tanaka, et al., "HDTV single-chip CCD color camera," IEEE Trans. Consumer Electron., vol. 36, pp. 479-485, Aug. 1990.

(5) S. N. Baron, and K. H. Powers, "Common image format for international television program exchange," 131st SMPTE Tech. Conf., Oct. 1989.

(6) E. G. Stevens, et al., "A 1-megapixel, progressive-scan image sensor with antiblooming control and lag-free operation," IEEE Trans. Electron Devices, vol. 38, pp. 981-988, May 1991.

(7) D. L. Losee, et al., "A 1/3" format image sensor with refractory metal light shield for color video applications," ISSCC Digest of Technical Papers, pp. 90-91, Feb. 1989

(8) M. Morimoto, et al., "A 2M pixel HDTV CCD image sensor with tungsten photo-shield and H-CCD shunt wiring," ISSCC Digest of Technical Papers, pp.172-173, Feb. 1992.

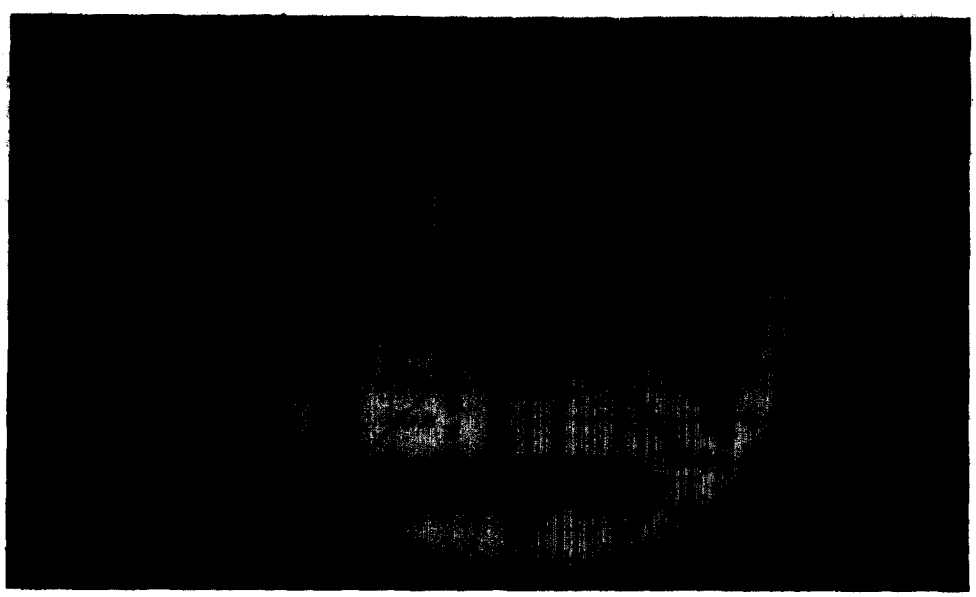

Fig. 9. Reproduced monochrome image captured by the sensor.

# KODAK KAI-2090CM Image Sensor
# Megapixel Interline CCD

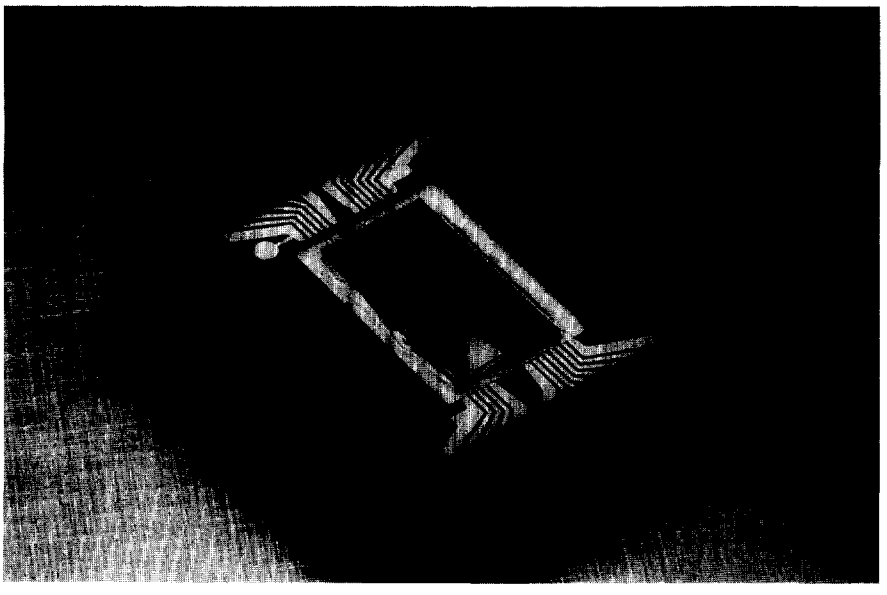

## *Description*

The Kodak KAI-2090CM is a single-chip color, high-definition television (HDTV) image sensor. This interlaced charge-coupled device (CCD) operates at video frame rates. It has square pixels and vertical-stripe color filter array for easier image processing. The photosensitive area has a 16:9 aspect ratio and is consistent with the "Common Image Format" (CIF). Applications for the device include HDTV, microscopy, and medical imaging.

| Parameter | Value |
|---|---|
| Architecture | Interline CCD, Interlaced |
| Photosensitive Pixels | 1928 (H) x 1084 (V) |
| Pixel Size | 7.3 µm (H) x 7.3 µm (V) |
| Photosensitive Area | 14.22 mm (H) x 7.97 mm (V) |
| Chip Size | 15.33 mm (H) x 8.62 mm (V) |
| Optical Fill-Factor | 55% |
| Saturation Signal | 45,000 electrons |

| Parameter | Value |
|---|---|
| Output Sensitivity | 8 µV/electron |
| Total Sensor Noise (1/30 sec readout, 1/30 sec integration) | 65 electrons rms |
| Dark Current | <.5 nA/cm² |
| Quantum Efficiency (λ=450, 530, 650 nm) | 33%, 32%, 25% |
| Blooming Suppression | 200 X |
| Maximum Data Rate | 38 MHz/Channel (2 channels) |
| Image Lag (First Field) | Negligible |

All parameters above are specified at T=40°C

EFFECTIVE DATE: JULY 1, 1993

## *Defect Classifications*

| Class | Point Defects Major | Point Defects Minor | Cluster Defects Total | Column Defects Total |
|---|---|---|---|---|
| C0 | 0 | 0 | 0 | 0 |
| C1 | ≤ 5 | ≤ 50 | 0 | 0 |
| C2 | ≤10 | ≤100 | ≤4 | ≤2 |
| C3 | ≤20 | ≤200 | ≤8 | ≤4 |

**Major Defective Pixel**—A pixel whose signal deviates by more than 25 mV from the mean value of all active pixels under dark field condition or by more than 15% from the mean value of all active pixels under uniform illumination at 80% of saturation.

**Minor Defective Pixel**—A pixel whose signal deviates by more than 8 mV from the mean value of all active pixels under dark field condition.

**Point Defect**—An isolated defective pixel.

**Cluster Defect**—A group of 2 to 6 contiguous major defective pixels.

**Column/Row Defect**—A group of more than 6 contiguous major defective pixels along a single column or row.

**Notes:**
1. No row defects are allowed.
2. No chroma column defects are allowed.

EASTMAN KODAK COMPANY
Building 81, Floor 5
Rochester, NY 14650-2010
Phone 716-722-4385
Fax 716-477-4947

**Test Conditions**

| | | |
|---|---|---|
| Junction Temperature | ($T_j$) | = 40°C |
| Integration Time | ($t_{int}$) | = 33msec |
| Readout Time | ($t_{readout}$) | = 33msec |

Kodak is a trademark.

*The world leader in imaging*

© Eastman Kodak Company, 1993 Printed in U.S.A. Specifications are subject to change without notification.

Dr. Thomas A. DeFanti
Chair, ACM SIGGRAPH Committee on ATV
tom@siggraph.org

RECEIVED
NOV 29 1993
FEDERAL COMMUNICATIONS COMMISSION
OFFICE OF THE SECRETARY

Position:

Progressive scan must be available on EVERY future television receiver so that the National Information Infrastructure can be built on the merger of digital television and digital computing.

Interlace does not give sufficient vertical resolution for NII usage. Hard-edge graphics and text need full vertical resolution with a flicker-free display. Interlace broadcast will result in unacceptable flicker on low-end receivers because progressive scan will not be mandated in these receivers.

Literacy and math skills are at stake. The NII is the key to the educational and life-long learning systems of the 21st century. We have unsuccessfuly struggled with bringing computers and television together for over 20 years, largely because of interlaced NTSC standards.

We are in a post-literate age. Without progressive scan as the lowest common denominator, it will be an illiterate age as well.